



CMS-SMP-21-002

CERN-EP-2022-013
2022/08/15

Measurement of the Drell–Yan forward-backward asymmetry at high dilepton masses in proton-proton collisions at $\sqrt{s} = 13$ TeV

The CMS Collaboration^{*}

Abstract

A measurement of the forward-backward asymmetry of pairs of oppositely charged leptons (dimuons and dielectrons) produced by the Drell–Yan process in proton-proton collisions is presented. The data sample corresponds to an integrated luminosity of 138 fb^{-1} collected with the CMS detector at the LHC at a center-of-mass energy of 13 TeV. The asymmetry is measured as a function of lepton pair mass for masses larger than 170 GeV and compared with standard model predictions. An inclusive measurement across both channels and the full mass range yields an asymmetry of $0.612 \pm 0.005\text{ (stat)} \pm 0.007\text{ (syst)}$. As a test of lepton flavor universality, the difference between the dimuon and dielectron asymmetries is measured as well. No statistically significant deviations from standard model predictions are observed. The measurements are used to set limits on the presence of additional gauge bosons. For a Z' boson in the sequential standard model the observed (expected) 95% confidence level lower limit on the Z' mass is 4.4 TeV (3.7 TeV).

Published in the Journal of High Energy Physics as doi:10.1007/JHEP08(2022)063.

1 Introduction

Drell–Yan (DY) production of pairs of same-flavor, oppositely charged leptons ($\ell^+ \ell^-$) in proton-proton (pp) collisions occurs via the s -channel exchange of Z/γ^* bosons. At leading order (LO) in quantum chromodynamics (QCD), the Z/γ^* bosons are produced via quark-antiquark ($q\bar{q}$) annihilation. The presence of both vector and axial couplings of gauge bosons to leptons results in a forward-backward asymmetry, A_{FB} , in the angular distribution of the final-state lepton with respect to the initial-state quark. Deviations from the standard model (SM) predictions of A_{FB} can result from the presence of an additional neutral gauge boson (Z') [1–7], quark-lepton compositeness [8], large extra dimensions [9], vector-like fermions [10], certain dark matter candidates [11], or leptoquarks [12]. Hints of a violation of lepton flavor universality in several measurements recently reported by the LHCb Collaboration [13–15] have sparked interest in models for physics beyond the SM that could explain these effects. Many of these models include heavy neutral gauge bosons or leptoquarks with non-flavor-universal couplings [16, 17], which could produce signatures in high-mass dilepton distributions [18]. As compared to measurements of differential cross sections at high dilepton masses, measurements of A_{FB} have a reduced dependence on systematic uncertainties related to the reconstruction and identification of high-momentum leptons. Hence, precision measurements of A_{FB} can provide stringent tests of the electroweak sector of the SM and of lepton flavor universality. The main results of this paper are measurements of A_{FB} as a function of dilepton mass for both muons and electrons in the high-mass region ($>170\,\text{GeV}$), which is particularly sensitive to potential contributions from new physics.

The asymmetry is defined in terms of the angle θ between the negatively charged final-state lepton and the initial-state quark (meant here in contrast to the antiquark) in the $\ell^+ \ell^-$ center-of-mass frame,

$$A_{\text{FB}} = \frac{\sigma_F - \sigma_B}{\sigma_F + \sigma_B}, \quad (1)$$

where σ_F (σ_B) is the total cross section for forward (backward) events, defined by $\cos \theta > 0$ (<0). The sign of θ is defined so that $\cos \theta = 1$ events are those in which the negatively charged final-state lepton is traveling in the same direction as the incident quark. The A_{FB} value can also be directly related to the parton-level differential cross section. The latter can be written as [19, 20]:

$$\frac{d\sigma}{d \cos \theta} \propto \frac{3}{8} \left[1 + \cos^2 \theta + \frac{A_0}{2} (1 - 3 \cos^2 \theta) + A_4 \cos \theta \right], \quad (2)$$

where A_0 and A_4 are the standard dimensionless constants parameterizing the angular distribution of the DY process [19, 20]. The terms that are functions of $\cos \theta$ with even parity do not contribute to A_{FB} , leading to the relation:

$$\frac{3}{8} A_4 = A_{\text{FB}}. \quad (3)$$

This form of the angular distribution is general for any s -channel processes mediated by a spin-1 boson and is thus applicable in the case of interference from additional heavy vector bosons. The angular coefficients A_0 and A_4 vary as functions of the mass (m), transverse momentum (p_T), and rapidity (y) of the dilepton system. As the dilepton transverse momentum approaches zero, A_0 vanishes. It is nonzero for finite $Z/\gamma^* p_T$ caused by processes in which Z/γ^* bosons are produced in association with additional jets. Thus, measurements of A_0 probe higher-order corrections in perturbative QCD. Additional results of this paper are the measurements of A_0 as a function of the dilepton mass in the same high-mass region ($>170\,\text{GeV}$).

Electroweak interference between the photon and the Z boson leads to negative values of A_{FB} with large absolute value for masses below the Z pole ($m < 80 \text{ GeV}$), and leads to large and positive values of A_{FB} above the Z pole ($m > 110 \text{ GeV}$). Near the Z boson mass peak, A_{FB} reflects pure Z exchange and is close to zero because of the small value of the charged-lepton vector coupling to Z bosons. In the high-mass region, above the Z boson peak, the SM value of A_{FB} is approximately constant with a value of ≈ 0.6 . The A_0 coefficient is expected to be ≈ 0.06 at 170 GeV and should decrease at higher masses.

For the case of a new heavy Z' , off-shell interference can produce deviations at masses significantly lower than the Z' mass. The deviation from the SM A_{FB} is insensitive to the width of the Z' [6, 7]. This measurement thus offers a complementary approach to previous searches for new physics in the dilepton channel that have searched for a peak in the invariant mass distribution caused by the resonant production of a new particle [21, 22]. Additionally, because the constraining power of this technique is based on interference rather than direct production, its sensitivity to higher mass scales is not limited by the center-of-mass energy and will continuously improve with the increased statistical precision with the addition of future LHC data.

When the dilepton system has nonzero p_T , the exact directions of the incident partons are unknown since they are no longer collinear with the proton beams. To minimize the impact of this effect on the asymmetry measurement, the Collins–Soper rest frame [23] is used. In this frame, θ^* is defined as the angle between the negatively charged lepton and the axis that bisects the angle between the incident parton directions. Approximating the leptons as massless, $\cos \theta^*$ can be computed from lab frame variables as:

$$\cos \theta^* = \frac{2(P_1^+ P_2^- - P_1^- P_2^+)}{m \sqrt{m^2 + p_T^2}}, \quad (4)$$

with

$$P_i^\pm = \frac{1}{\sqrt{2}}(E_i \pm p_{z,i}),$$

where E_i is the energy and $p_{z,i}$ the longitudinal momentum of the lepton ($i = 1$) and antilepton ($i = 2$). The sign of $\cos \theta^*$ is defined with respect to the direction of the incident quark, which is unknown for collisions in a pp collider. Typically, the quarks in the collision will carry a larger momentum fraction than the antiquarks, since only the quarks are valence partons of protons. Thus, usually the lepton pair will have longitudinal momentum along the direction of the incident quark. Therefore, instead of using the initial quark direction, one can define the positive axis to be the longitudinal direction of the lepton pair. We denote the angular variable defined in this way as:

$$\cos \theta_R = \frac{p_z}{|p_z|} \cos \theta^*. \quad (5)$$

where p_z is the longitudinal momentum of the dilepton system. The presence of events where the quark direction does not match the lepton pair direction dilutes the asymmetry observed in $\cos \theta_R$ as compared with the underlying asymmetry in $\cos \theta^*$. The fraction of events for which the quark direction is the same as the longitudinal momentum of the lepton pair increases with the absolute value of the dilepton rapidity. At an invariant mass of 500 GeV, this fraction is $\approx 60\%$ at $|y| = 0.2$ and $\approx 95\%$ at $|y| = 2$.

The asymmetry, A_{FB} , was previously measured by the CMS Collaboration at $\sqrt{s} = 7 \text{ TeV}$ [24] and 8 TeV [25] and by the ATLAS Collaboration at $\sqrt{s} = 7 \text{ TeV}$ [26]. Around the Z boson peak,

measurements of A_{FB} have been used by CMS and ATLAS to extract the effective weak mixing angle $\sin^2\theta_{\text{eff}}^\ell$ [26, 27]. The results presented in this paper at $\sqrt{s} = 13 \text{ TeV}$ takes a new approach to measuring A_{FB} . Rather than counting forward and backward events, A_{FB} is extracted by fitting a set of templates constructed to represent the different terms in Eq. (2) to the measured angular distribution. These templates are constructed from Monte Carlo (MC) simulations, which include the dilution effect. The A_{FB} measured by the template fitting method corrects for the dilution effect and thus determines the asymmetry in $\cos\theta^*$, whereas the A_{FB} measured by the traditional counting method does not correct for the dilution and determines the asymmetry in $\cos\theta_R$. Additionally, the template-based measurement of A_{FB} optimally combines the information from the full fiducial dilepton rapidity range into a single measurement, rather than being reported differentially in rapidity as is done in the counting method. This means that the A_{FB} values from this measurement are not directly comparable with the previous CMS results. The previous ATLAS publication utilized the counting method but also included additional results unfolding the dilution effect, that are comparable with this measurement. This template-based measurement is a maximum-likelihood estimate of A_{FB} and leads to a $\approx 20\%$ smaller uncertainty than a simple counting-based measurement [28]. However it relies more heavily on parton distribution functions, and cannot be as easily reinterpreted using new models as a counting-based measurement of the diluted A_{FB} .

2 Analysis strategy

The observed distribution of the reconstructed scattering angle, $\cos\theta_R$, abbreviated as c_R , can be expressed as a convolution of the $\cos\theta^*$, abbreviated c_* , distribution defined in Eq. (2),

$$f(c_R) = C \int dc_* R(c_R; c_*) \varepsilon(c_*) \frac{d\sigma}{dc_*}, \quad (6)$$

where C is a normalization constant, R is a “reconstruction function” that incorporates detector resolution and the dilution effect, and ε is an efficiency function. It is important to point out that convolutions are linear operations, which implies that the resulting reconstructed distribution can be expressed as a sum of convolutions of each of the terms in Eq. (2).

This linearity allows the fitting function to be represented by a set of parameter-independent templates corresponding to the different terms in Eq. (2). By fitting the observed data distribution to combinations of these signal templates and additional background templates, one can extract A_{FB} and A_0 . The DY signal templates, representing the reconstructed angular distribution corresponding to each of the terms in the true angular distribution of Eq. (2), are constructed by reweighting MC simulated events. The details of the signal template construction are discussed in Section 7.

The templates for the dominant backgrounds are extracted from MC simulation and validated in a control region of $e\mu$ events. Templates for additional backgrounds that are not well modeled by MC are constructed based on control samples in data.

Because the form of Eq. (2) is general for any s -channel spin-1 process, the measured values of A_{FB} can be used to set limits on the existence of heavy Z' bosons.

To search for signs of lepton flavor universality violation, the difference between A_{FB} and A_0 in the muon and electron channels can be measured directly. The parameters of interest in these measurements are $\Delta A_{\text{FB}} = A_{\text{FB},\mu\mu} - A_{\text{FB},ee}$ and $\Delta A_0 = A_{0,\mu\mu} - A_{0,ee}$. The direct measurement of ΔA_{FB} is less sensitive to systematic uncertainties common to the muon and electron channels

than the measurement of A_{FB} in the individual channels, and thus has reduced systematic uncertainty.

Fiducial corrections and measurement interpretation

In this analysis, A_{FB} and A_0 are measured as functions of the dilepton mass, but A_{FB} and A_0 also depend on the dilepton p_{T} and rapidity. A single A_0 parameter and a single A_{FB} parameter are measured in each mass bin, representing effective values, integrated over p_{T} and rapidity. However, because the acceptance of dilepton events in the CMS detector is not independent of the dilepton p_{T} and rapidity, the effective A_0 or A_{FB} of recorded events is not the same as the effective value in the full phase space. The effect was studied in MC simulations and it was found that differences between the fiducial and full phase space values of A_0 were insignificant, but the differences in A_{FB} could be as large as 2% in the lower mass bins. Using these MC simulations, a correction factor was derived to convert the fiducial A_{FB} directly measured in the data to that of the full phase space. This correction factor is then applied to the result of the template fit so that the final reported value is a measurement of the A_{FB} in the full phase space. Uncertainties in the MC simulation are propagated through the evaluation of this correction factor, and are treated as a source of systematic uncertainty in the final measurement.

This template fitting technique automatically accounts for all other resolution, dilution, migration, and acceptance effects since they are modeled in the simulation. Uncertainties in the simulation of these effects can be accounted for using variations of the corresponding templates, as discussed in Section 8. The final result can thus be interpreted as a measurement of the partonic A_{FB} in different bins of the reconstructed lepton pair mass. Because the mass bins used are large and the SM A_{FB} is essentially independent of the dilepton mass in the high-mass region of our measurement, the measurement is not unfolded to parton-level mass bins.

3 The CMS detector and physics objects

The central feature of the CMS apparatus is a superconducting solenoid of 6 m internal diameter, providing a magnetic field of 3.8 T. Within the solenoid volume are a silicon pixel and strip tracker, a lead tungstate crystal electromagnetic calorimeter (ECAL), and a brass and scintillator hadron calorimeter (HCAL), each composed of a barrel and two endcap sections. Forward calorimeters extend the pseudorapidity (η) coverage provided by the barrel and endcap detectors. Muons are detected in gas-ionization chambers embedded in the steel flux-return yoke outside the solenoid. A more detailed description of the CMS detector, together with a definition of the coordinate system used and the relevant kinematic variables, is reported in Ref. [29].

Events of interest are selected using a two-tiered trigger system. The first level, composed of custom hardware processors, uses information from the calorimeters and muon detectors to select events at a rate of around 100 kHz within a fixed latency of about 4 μs [30]. The second level, known as the high-level trigger, consists of a farm of processors running a version of the full event reconstruction software optimized for fast processing, and reduces the event rate to around 1 kHz before data storage [31].

The particle-flow algorithm [32] aims to reconstruct and identify each individual particle in an event, with an optimized combination of information from the various elements of the CMS detector. The energy of photons is obtained from the ECAL measurement. The energy of electrons is determined from a combination of the electron momentum at the primary interaction vertex as determined by the tracker, the energy of the corresponding ECAL cluster, and the energy sum of all bremsstrahlung photons spatially compatible with originating from the elec-

tron track. The energy of muons is obtained from the curvature of the corresponding track. The energy of charged hadrons is determined from a combination of their momentum measured in the tracker and the matching ECAL and HCAL energy deposits, corrected for the response function of the calorimeters to hadronic showers. Finally, the energy of neutral hadrons is obtained from the corresponding corrected ECAL and HCAL energies. The candidate vertex with the largest value of summed physics-object p_T^2 is assigned to be the primary pp interaction vertex. The physics objects are the jets, clustered using the anti- k_T jet finding algorithm [33, 34] with the tracks assigned to candidate vertices as inputs.

Muons are measured in the range $|\eta| < 2.4$, with detection planes made using three technologies: drift tubes, cathode strip chambers, and resistive-plate chambers. The single-muon trigger efficiency exceeds 90% over the full η range, and the efficiency to reconstruct and identify muons is greater than 96%. Matching muons to tracks measured in the silicon tracker results in a relative p_T resolution of 1% in the barrel and 3% in the endcaps for muons with p_T up to 100 GeV, and of better than 7% for muons in the barrel with p_T up to 1 TeV [35].

The single-electron trigger efficiency is approximately 80% over the full η range, and the efficiency to reconstruct and identify electrons is greater than 65% for electrons with $p_T > 20$ GeV. The momentum resolution for electrons with $p_T \approx 45$ GeV from $Z \rightarrow ee$ decays ranges from 1.7–4.5%. It is generally better in the barrel region than in the endcaps, and also depends on the bremsstrahlung energy emitted by the electron as it traverses the material in front of the ECAL [36].

Jets are clustered from the particle-flow candidates in an event using the anti- k_T jet finding algorithm with a distance parameter of 0.4. Jet momentum is determined as the vectorial sum of all particle momenta in the jet, and is found from simulation to be, on average, within 5–10% of the true momentum over the whole p_T spectrum and detector acceptance. Additional pp interactions within the same or nearby bunch crossings ("pileup") can contribute additional tracks and calorimetric energy depositions, increasing the apparent jet momentum. To mitigate this effect, tracks identified as originating from pileup vertices are discarded and an offset correction is applied to correct for remaining contributions [37]. Jet energy corrections are derived from simulation studies so that the average measured energy of jets becomes identical to that of particle level jets [38]. In situ measurements of the momentum balance in dijet, photon+jet, Z +jet, and multijet events are used to determine any residual differences between the jet energy scale in data and in simulation, and appropriate corrections are made [38]. The missing transverse momentum vector (\vec{p}_T^{miss}) is defined as the negative vector p_T sum of all the particle-flow candidates in an event, and its magnitude is denoted as p_T^{miss} [39]. The \vec{p}_T^{miss} is modified to account for corrections to the energy scale of the reconstructed jets in the event.

4 Data and Monte Carlo samples

The analysis is performed with pp collision data collected with the CMS detector at the LHC in 2016–2018 at $\sqrt{s} = 13$ TeV. The total integrated luminosity amounts to 138 fb^{-1} [40–42].

Various MC generators have been used to simulate the DY signal and background processes. The DY signal samples, $Z/\gamma^* \rightarrow ee$ and $Z/\gamma^* \rightarrow \mu\mu$, and the background sample $Z/\gamma^* \rightarrow \tau\tau$, have been generated at next-to-leading order (NLO) with MADGRAPH5_aMC@NLO [43] (shortened as aMC@NLO), using version v2.2.2 (v2.6.0) for samples corresponding to the 2016 (2017–2018) data-taking period. Up to two additional partons are allowed using the FxFx merging scheme [44]. The samples are interfaced with PYTHIA [45] to simulate the parton shower, hadronization, and quantum electrodynamics final-state radiation. The CUETP8M1 [46] (CP5 [47])

PYTHIA tune and PYTHIA version v8.226 (v8.230) are used for the samples corresponding to the 2016 (2017–2018) data-taking period. The NLO NNPDF 3.0 parton distribution functions (PDFs) [48, 49] are used for all three data-taking periods.

Other processes that can give a final state with two oppositely charged same-flavor leptons are diboson production (WW , WZ , ZZ), photon-induced dilepton production ($\gamma\gamma \rightarrow \ell\ell$), top quark pair production ($t\bar{t}$), and single top quark production in association with a W boson (tW). The $t\bar{t}$ and tW backgrounds are generated at NLO using POWHEG v2.0 [50–53], and interfaced to PYTHIA with the CUETP8M2T4 [54] (CP5) tune for the 2016 (2017–2018) data-taking period. Background samples of $ZZ \rightarrow \ell\ell\ell'\ell'$, $ZZ \rightarrow \ell\ell\nu\nu$, and $WW \rightarrow \ell\nu\ell\nu$ are generated at NLO with POWHEG interfaced to PYTHIA. Background samples of $WZ \rightarrow q\bar{q}\ell\ell$ and $ZZ \rightarrow q\bar{q}\ell\ell$ are generated at NLO with aMC@NLO interfaced to PYTHIA. The WW , WZ , and ZZ samples corresponding to the 2016 (2017–2018) data-taking period are interfaced with PYTHIA using the CUETP8M1 (CP5) tune. The $t\bar{t}$, tW , and diboson backgrounds corresponding to the 2016 (2017–2018) data-taking period use the NNPDF 3.0 (3.1) PDFs. The photon-induced background, $\gamma\gamma \rightarrow \ell\ell$, is simulated using the CEPGEN [55] implementation of LPAIR [56, 57], interfaced to PYTHIA v6.429 [58], and using the default proton structure function parameterization of Suri-Yennie [59]. This contribution is split into three parts because the interaction at each proton vertex can be elastic or inelastic.

The cross sections of WZ and ZZ diboson samples are normalized to the NLO predictions calculated with MCFM 6.6 [60], whereas the cross sections of the WW samples are normalized to the next-to-NLO (NNLO) predictions [61]. The total cross section of the $t\bar{t}$ process is normalized to the prediction with NNLO accuracy in QCD and next-to-next-to-leading-logarithmic accuracy for the soft gluon radiation resummation calculated with TOP++ 2.0 [62].

The detector response for all MC samples is simulated using a detailed description of the CMS detector based on GEANT4 [63]. The pileup distribution in simulation is weighted to match the one observed in data.

5 Event selection

Events are required to have two leptons of the same flavor and opposite charges. The dimuon and dielectron events are selected by single-muon and single-electron triggers, respectively. The thresholds of these triggers are different for the different data-taking years, and the leading muon or electron in the event is required to have a p_T above the trigger threshold. In the analysis, the leading muon p_T requirement for the years 2016/2017/2018 is 26/29/26 GeV and for electrons it is 29/38/35 GeV. The subleading lepton is required to have $p_T > 15$ GeV. All muons are required to be within the acceptance of the muon system ($|\eta| < 2.4$) and all electrons must be within $|\eta| < 2.5$, excluding the barrel-endcap transition region of the ECAL ($1.44 < |\eta| < 1.57$). Additionally, to remove cosmic-ray-induced events, the azimuthal angle (ϕ) between the two muons is required to differ from π by more than 5 mrad.

Each reconstructed muon is required to pass identification criteria that are based on the number of hits observed in the tracker, the response of the muon detectors, and a set of matching criteria between muon track parameters, as measured by the inner tracker and muon detectors. To suppress nonprompt muons coming from heavy-flavor decays, both muons must be isolated from other particles in a cone of size $\Delta R = 0.3$, where $\Delta R = \sqrt{(\Delta\eta)^2 + (\Delta\phi)^2}$ refers to the distance from the muon to a given track. More details on the muon identification and reconstruction used in this analysis can be found in Refs. [35, 64].

The reconstructed electron candidates are required to pass identification criteria that are based on electromagnetic shower shape variables. Electrons originating from photon conversions are suppressed by requiring that the candidates have at most one missing inner tracker hit and are not consistent with being part of a conversion pair. Electrons are also required to be isolated from other particles within a cone of size $\Delta R = 0.3$. The electron isolation criteria are based on the ratio of the electron p_T to the sum of energy deposits associated with the photons as well as with the charged and neutral hadrons reconstructed by the particle-flow algorithm. More details on the electron reconstruction and identification criteria used in this analysis are described in Ref. [36].

To suppress backgrounds that contain the decays of top quarks, two additional requirements are applied. First, events are required to have $p_T^{\text{miss}} < 100 \text{ GeV}$. Second, it is required that neither of the two highest p_T jets in the event with $|\eta| < 2.4$ are identified as a bottom quark jet (b tagged). Jets originating from decays of bottom quarks are identified using an algorithm that combines lifetime information from tracks and secondary vertices [65]. A working point is used that has a 68% efficiency of correctly identifying a bottom quark jet and a 1% probability of misidentifying a light-flavor quark or gluon jet as a bottom quark jet.

6 Backgrounds

At large lepton pair masses, the dominant background comes from fully leptonic decays of $t\bar{t}$ events. There are also backgrounds from tW events, diboson processes and $\tau\tau$ leptonic decays. All of these backgrounds are well modeled in simulation, and the estimated event yields are validated in data in a control region of $e\mu$ events. Multijet and $W+\text{jets}$ events where one or more jets are incorrectly identified as leptons (denoted as “MisID” events) are also a source of background. This background is larger for the ee channel than for the $\mu\mu$ channel. A technique based on control samples in data is employed to estimate this background. There are also backgrounds coming from t -channel photon-induced dilepton production, which are modeled with MC simulation as well.

The MisID background is estimated from data using the “misidentification rate” method. Descriptions of this method are reported in Refs. [66, 67]. The misidentification rate is defined as the probability of a jet, having been reconstructed as a lepton candidate, to pass the lepton selection requirements. This rate is measured in a sample with two leptons coming from a Z boson decay and an additional, potentially misidentified, lepton. These two leptons are required to pass the lepton identification requirements and have an invariant mass within 7 GeV of the Z boson mass [68]. The presence of the third lepton candidate is used as a probe to measure the misidentification rate. These lepton candidates are required to pass a set of identification and isolation requirements less stringent than the full selection requirements of the analysis. The MisID background can then be estimated from a sample of data events with two lepton candidates where at least one of the candidates fails the full selection requirements. Events from this sample are assigned weights based on the expected misidentification probability of the failing lepton candidates. Contamination of this sample by lepton pairs from DY and other prompt processes is subtracted using MC simulation. These reweighted events are used to estimate the yield and shape of the MisID background.

This method of background estimation is validated in a control region. This control region has all the same selection criteria and covers the same dilepton mass range ($m > 170 \text{ GeV}$) as the signal region except the lepton pairs are required to have same-sign rather than opposite-sign charges. A large fraction of the events in this control region stem from misidentified jets. In the ee channel, there is also a significant contribution to this sample from opposite-sign DY

events where one of the electrons has had its charge incorrectly assigned. The rate of this misassignment is not modeled well in simulation, and so a correction to the MC is derived in the mass window of the Z peak ($70 < m < 110$ GeV) and applied. The MisID background estimate as well as MC estimates of other backgrounds are compared with the observed yield of same-sign events. A $\cos \theta_R$ -dependent correction to the MisID background estimate is derived using the ratio of the MisID estimate to the number of observed same-sign events minus other backgrounds. The uncertainty in this correction is calculated as the quadratic sum of the statistical uncertainties from the limited sample size, uncertainty in the amount of DY pairs reconstructed as same-sign pairs, as well as systematic uncertainty reflecting possible differences in shape between same-sign and opposite-sign MisID estimates.

Because the $\tau\tau$, tW , $t\bar{t}$, and diboson backgrounds all have decays to $e\mu$ pairs as well, the MC simulation of these processes can be validated in data. The $e\mu$ control region used has all the same selection criteria as the signal region, except that events are required to have one muon and one electron rather than a pair of the same flavor. The muon is required to have $p_T > 26/29/26$ GeV for the years 2016/2017/2018 and pass the muon trigger used in the main analysis, and the electron is required to have $p_T > 15$ GeV. There are also MisID events in this $e\mu$ control region coming from QCD multijet and W+jets backgrounds. These are estimated using the misidentification rate technique previously described. The dilepton invariant mass and $\cos \theta_R$ distributions of $e\mu$ events are shown in Fig. 1. Good agreement is observed between the simulated and observed yield of $e\mu$ events across the entire mass range.

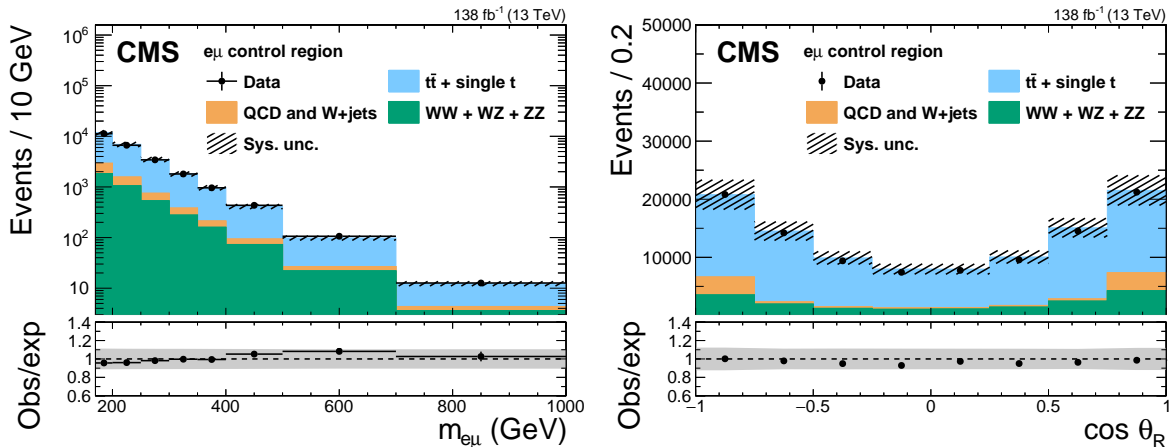


Figure 1: The invariant mass distribution (left) and $\cos \theta_R$ distribution (right) of $e\mu$ events observed in CMS data (black dots with statistical uncertainties) and expected backgrounds (stacked histograms). The hatched bands show the systematic uncertainty in the expected yield. The sources of this uncertainty are discussed in Section 8. The lower panels show the ratio of the data to the expectations. The gray bands represent the total uncertainty in the predicted yields.

Because diboson events are produced via electroweak processes, they are expected to have a small forward-backward asymmetry in their lepton pairs; $t\bar{t}$ events are also known to have an asymmetry, but it is too small to be detected in its lepton pairs alone [69]. The QCD and W+jets backgrounds should have no asymmetry. Based on MC and control sample estimates, we predict an overall forward-backward asymmetry of ≈ 0.01 in the sample of $e\mu$ events. Using the definition in Eq. (1), the A_{FB} of the $e\mu$ sample is found to be 0.012 ± 0.003 , consistent with this expectation.

Although the overall normalizations and asymmetries of the MC $e\mu$ estimates are observed to be consistent with data, there are discrepancies between the predicted and observed shapes

of the $\cos \theta_R$ distribution in certain ranges of dilepton mass. To address these discrepancies, a $\cos \theta_R$ correction is derived from the $e\mu$ sample in data, based on the ratio of the observed and predicted $\cos \theta_R$ distributions. Because the asymmetry is modeled well, this correction is derived symmetrically in $\cos \theta_R$ using four bins of $|\cos \theta_R|$. To account for the changing $\cos \theta_R$ shapes as a function of the dilepton mass, the correction is derived separately in different mass bins. Corrections are derived in five mass bins (170, 200, 250, 320, 510, 3000 GeV) with edges matching those used in the A_{FB} measurement (defined in Section 7), combining the highest mass bins because of a limited event count. These corrections are applied to modify the shapes of the templates used to model the corresponding backgrounds in the signal region. They change the estimated $\cos \theta_R$ shape of these backgrounds and introduce uncertainties in these shapes at the level of by $\approx 5 \pm 4\%$ and $\approx 15 \pm 10\%$ in the lowest and highest mass bins, respectively.

Figure 2 shows a comparison between measured $\mu\mu$ and ee events and our estimates in the signal region after all corrections have been applied. Good agreement is observed between the simulated and observed amount of $\mu\mu$ and ee events.

7 Template construction

From the MC sample of DY events, templates for each of the three terms in Eq. (2) need to be constructed. To avoid any of the templates having a negative yield in any of the bins, two reparameterizations are performed. The angular distribution is rewritten in a slightly different form than Eq. (2):

$$\frac{d\sigma}{dc_*} \propto \frac{3}{4(2+\alpha)} \left[1 + c_*^2 + \alpha(1 - c_*^2) + \frac{4(2+\alpha)}{3} A_{FB} c_* \right]. \quad (7)$$

This form is equivalent to Eq. (2) for $\alpha = 2A_0/(2 - A_0)$. The term corresponding to NLO QCD production ($1 - c_*^2$) is now strictly positive.

The three templates, f_S , f_α , and f_A , can now be constructed to represent the $1 + c_*^2$, $1 - c_*^2$, and c_* terms in Eq. (7). These templates are constructed by reweighting MC events using generator-level quantities but are binned in the reconstructed variables. Note that the generator-level c_* and the reconstructed c_R can have different signs. To minimize the impact of statistical fluctuations in our MC simulations, each event is used twice in the template construction. Each event is used once with $+c_*$ and once with $-c_*$, and each use is given half weight to keep the normalization unchanged. The following reweighting factors are used to construct the f_S , f_α , and f_A templates respectively:

$$w_S(|c_*|) = \frac{1 + c_*^2}{1 + c_*^2 + \alpha(1 - c_*^2)}, \quad (8)$$

$$w_\alpha(|c_*|) = \frac{1 - c_*^2}{1 + c_*^2 + \alpha(1 - c_*^2)}, \quad (9)$$

$$w_A(c_*) = \frac{c_*}{1 + c_*^2 + \alpha(1 - c_*^2)}. \quad (10)$$

The α values in the denominator are extracted from fits to generator level distributions of our MC simulation events.

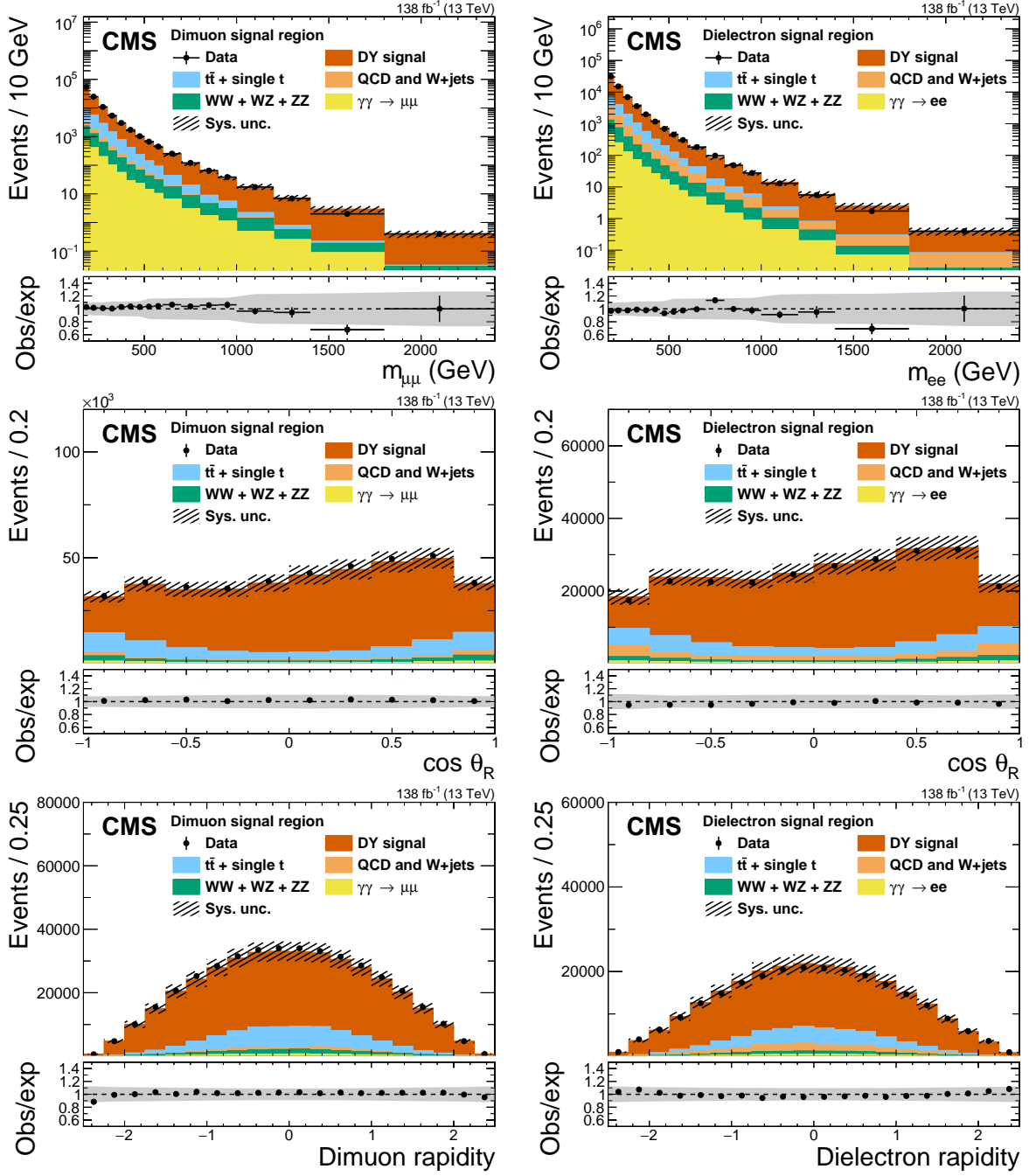


Figure 2: A comparison of CMS data and expected signal and background distributions in dilepton invariant mass (upper row), $\cos \theta_R$ (middle row) and dilepton rapidity (lower row). The left plot shows the $\mu\mu$ channel and the right plot the ee channel. The black points with error bars represent the data and their statistical uncertainties, whereas the combined signal and background expectation is shown as stacked histograms. The hatched band shows the systematic uncertainty in the expected signal and background yield. The sources of this uncertainty are discussed in Section 8. The lower panels show the ratio of the data to the expectation. The gray bands represents the total uncertainty in the predicted yield.

Then a histogram of CMS data events, f_{data} , could be parameterized by:

$$f_{\text{data}} = \sum_j f_{\text{bkg}}^j + N(\alpha) \left[\alpha f_\alpha + f_S + \frac{A_{\text{FB}}}{N(\alpha)} f_A \right], \quad (11)$$

where the normalization factor $N(\alpha) = 3/[4(2 + \alpha)]$ has been introduced for convenience and f_{bkg}^j represents templates for the different backgrounds.

To avoid the negative values of the antisymmetric template (f_A), two positive-valued linear combinations of f_A and f_S , are constructed as:

$$f_S + \frac{A_{\text{FB}}}{N(\alpha)} f_A = (1 + \frac{A_{\text{FB}}}{N(\alpha)}) \frac{f_S + f_A}{2} + (1 - \frac{A_{\text{FB}}}{N(\alpha)}) \frac{f_S - f_A}{2} \equiv (1 + \frac{A_{\text{FB}}}{N(\alpha)}) f_+ + (1 - \frac{A_{\text{FB}}}{N(\alpha)}) f_-.$$
(12)

Then CMS data in each mass bin can be fit by the following parameterization:

$$f_{\text{data}} = \sum_j f_{\text{bkg}}^j + N(\alpha) \left[\alpha f_\alpha + (1 + \frac{A_{\text{FB}}}{N(\alpha)}) f_+ + (1 - \frac{A_{\text{FB}}}{N(\alpha)}) f_- \right], \quad (13)$$

where the asymmetry A_{FB} and α are allowed to float.

Separate templates are made for seven different mass bins to facilitate the extraction of the A_{FB} and A_0 coefficients as functions of mass. The bin edges used (in units of GeV) are: 170, 200, 250, 320, 510, 700, 1000 and infinity, where the last bin contains all events with dilepton mass greater than 1000 GeV.

Within each mass bin, the two-dimensional (2D) templates are binned in c_R and lepton pair rapidity $|y|$. Because of the acceptance effects, there are very few events with high rapidity and large $|c_R|$. Therefore, a different c_R binning is adopted at high rapidity. There are four bins in $|y|$ with bin edges at: 0.0, 0.6, 1.0, 1.5, and 2.4. For $|y| < 1.0$, there are eight uniform c_R bins from -1.0 to 1.0. For $|y| > 1.0$, the pairs of bins with $|c_R| > 0.5$ are merged leaving six c_R bins in this region. Additionally, there are few events with large rapidity at high mass so for the highest two mass bins (700–1000 and >1000 GeV) the two rapidity bins with $|y| > 1.0$ are merged leaving three $|y|$ bins in this region.

There are several templates for various background processes. Because of their similar shapes and the small magnitude of the tW background, the top quark related background processes ($t\bar{t}$, tW) are combined into a single background template. Diboson backgrounds (WW, ZZ, WZ) are combined into a single background template as well. The $\gamma\gamma \rightarrow \ell\ell$ process is a separate background template and constitutes 1–4% of the total cross section in the mass range of the measurement. The MisID estimate is also included as a separate background template. A $Z/\gamma^* \rightarrow \tau\tau$ template is included as well. To minimize statistical fluctuations, the templates for the top and MisID backgrounds are symmetrized in $\cos\theta_R$. The templates for the diboson, $Z/\gamma^* \rightarrow \tau\tau$, and $\gamma\gamma \rightarrow \ell\ell$ processes are not symmetrized because these processes have perceptible asymmetries.

Differential measurements of A_{FB} and A_0 are performed by fitting each mass bin independently, with a set of nuisance parameters uncorrelated with those in other mass bins. The results of an inclusive measurement in which all mass bins ($m > 170$ GeV) are fit simultaneously is also reported. Within each mass bin all three years are fit simultaneously as separate categories. Two sets of fits are performed to extract A_{FB} and A_0 : one in which the A_{FB} and A_0 parameters in the ee channel and $\mu\mu$ channels are allowed to float independently, and one in which they are fit with common A_{FB} and A_0 parameters. An additional set of fits is performed to extract ΔA_{FB}

and ΔA_0 . In these fits, the A_{FB} and A_0 parameters in the ee channel are used as a reference and the A_{FB} and A_0 parameters in the $\mu\mu$ channel are constructed in relation to them using the definitions of ΔA_{FB} and ΔA_0 . The A_{FB} and A_0 values in the ee channel are allowed to freely float in the measurements of ΔA_{FB} and ΔA_0 . These measurements of ΔA_{FB} and ΔA_0 are performed separately for each mass bin, as well as inclusively across all mass bins.

8 Systematic uncertainties

Systematic uncertainties in the normalization and shape of templates arise from a variety of sources and are defined through nuisance parameters in the likelihood. For systematic uncertainties that can change the shape of a template, shifted templates are constructed by varying the source of the systematic uncertainty up and down within its uncertainty. Shape uncertainties are incorporated into the likelihood by interpolation between the nominal and shifted templates, constrained with a Gaussian prior. The interpolation is calculated with a sixth-order polynomial for shifts smaller than one Gaussian σ , and with a linear function for shifts beyond one Gaussian σ . Normalization uncertainties are included using log-normal priors.

PDFs: variations in PDFs can change the dilution factor and kinematic distributions of the MC simulation samples. The 100 NNPDF set replicas are converted to 60 Hessian eigenvector variations [70]. For each of these 60 variations an “up” template is constructed using the variation’s weight. A “down” template is then constructed that symmetrizes the deviation from the nominal template. Each variation is treated as a separate shape uncertainty yielding 60 nuisance parameters associated with PDFs in the fit.

MisID background estimate: the uncertainty in the normalization of the MisID background and the uncertainty in the shape of the MisID $\cos \theta_R$ distribution are considered separately. Their normalizations are assigned a 50% uncertainty based on closure studies of the misidentification rate technique performed in simulation. The uncertainties in the shape corrections come from the statistical uncertainties of the same-sign validation and systematic uncertainties reflecting the shape differences between the same-sign and opposite-sign MisID estimates.

Lepton efficiencies: scale factors are derived and applied to the simulated MC events to account for the differences in the detector performance between CMS data and the MC simulation. The efficiencies for the trigger, lepton identification, and lepton isolation are measured as functions of lepton p_T and η using the “tag-and-probe” [35, 36] method for both data and simulation. For muons, separate uncertainties are included for the muon trigger, identification, and isolation efficiencies, with the uncertainty in reconstruction efficiency being negligible. For electrons, isolation is part of the identification requirements rather than a separate selection, so separate uncertainties are included for the electron trigger, reconstruction, and identification/isolation efficiencies. The efficiency uncertainties also include the effects of timing issues in the ECAL endcaps and muon chambers that caused inefficiencies in the first-level trigger in the range of 0–3% for the different data-taking periods. For each of these uncertainties, up and down templates are constructed from MC simulations using the up and down values from the uncertainty in the scale factors.

Lepton scale corrections: the muon momentum and electron energy scales can be affected by detector alignment and imperfect calibration. Such issues are corrected by additional energy and momentum scale corrections applied to both simulation and data. A bias in the muon momentum reconstruction can occur because of the differences in the tracker alignment between CMS data and simulation, as well as a residual magnetic field mismodeling. The muon momentum scale corrections are applied using the procedure described in Refs. [64, 71]. The

electron energy deposits, as measured in the ECAL, are subject to a set of corrections involving information from both the ECAL and tracker [36]. Separate up and down templates are constructed for the electron smearing, and muon and electron scales based on the uncertainty of these corrections.

Cross sections: a systematic uncertainty is attributed to the normalization of signal and background samples estimated by MC event generators. Based on NNLO calculations using the FEWZ v3.1 simulation code [72], a 3% uncertainty is assigned to the DY cross section. Based on NLO calculations, a 5% uncertainty is attributed to the backgrounds from top quark decays [62], and a 4% uncertainty in the diboson backgrounds [61, 73, 74]. A 6% uncertainty is attributed to the normalization of the $\gamma\gamma \rightarrow \ell\ell$ background, and it has been verified that this value covers the differences of samples generated using Suri–Yennie structure functions and the LuxQED [75, 76] photon PDFs.

Statistical uncertainties in templates: we treat the uncertainty due to the finite number of MC events, as well as the finite number of data events used to build the MisID templates, using a modified “Barlow–Beeston–like” approach [77], which adds a Gaussian uncertainty reflecting the number of events accumulated in each template bin. However, template bins at $\pm \cos \theta_R$ have partially correlated uncertainties because of events being used multiple times in the construction of signal, MisID background, and top quark background templates, but not reused in the $\gamma\gamma \rightarrow \ell\ell, \tau\tau$, and diboson background templates. To account for this correlation, additional constraint terms are added in the fit. These additional terms constrain the differences in the Barlow–Beeston–like nuisance parameters in correlated bins with Gaussian constraints. For each channel and mass bin, the correlation coefficient between bins at $\pm \cos \theta_R$ is computed and the standard deviation of the Gaussian function chosen conservatively based on the maximum amount of uncorrelated uncertainty in each mass bin. Based on the computed correlations, a variance of 0.1 is used for the Gaussian constraints on the template bins in the first four mass bins, and a variance of 0.6 for the Gaussian constraints on template bins in the highest three mass bins.

Integrated luminosity: the integrated luminosities of the 2016, 2017, and 2018 data-taking periods are individually known with uncertainties in the 1.2–2.5% range [40–42], while the total 2016–2018 integrated luminosity has an uncertainty of 1.6%, the improvement in precision reflecting the (uncorrelated) time evolution of some systematic effects.

Renormalization + factorization scale and strong coupling: the renormalization (μ_R) and factorization scales (μ_F), and strong coupling (α_S) used in MC generation can also have an effect on the shape and normalization of the templates. The μ_R and μ_F uncertainties are included by reweighting simulated events to match alternative scenarios where μ_R and μ_F are scaled up and down by a factor of two, both independently and simultaneously. The unphysical combinations where μ_R and μ_F are scaled in opposite directions are not included. Three nuisance parameters, describing μ_R , μ_F and combined μ_R and μ_F scale variations are included in the fit and are taken to be uncorrelated with respect to each other. Simulated events are also reweighted to account for variations of α_S and used to construct up and down templates. A central value of $\alpha_S = 0.118$ and variations of ± 0.0015 are used [78].

Background shape corrections: as discussed in Section 6, a shape correction based on $e\mu$ data events is applied to MC simulation derived backgrounds from top quarks and diboson events. The uncertainties in this shape correction are modeled with four independent nuisance parameters. Each parameter allows the values of the shape correction in a particular $|\cos \theta_R|$ bin to vary up and down within its statistical uncertainty.

DY p_T correction: it is known that the DY dilepton p_T spectrum is difficult to model at low p_T [79, 80]. Because acceptance is correlated with p_T , mismodeling of the p_T spectrum can result in mismodeling of the DY contribution. For this reason, the DY MC p_T spectrum in each mass bin is corrected based on data. For each mass bin used in the measurement, the normalized DY MC simulation p_T distribution is compared with the normalized data distribution, less the contributions from backgrounds. A correction factor is then derived based on the ratio of these two distributions. When building the templates used in the measurement, events are reweighted with this additional factor so that the events used to build the templates match the p_T spectrum of data events. To model the uncertainty in this correction seven separate nuisance parameters are used, one for each p_T bin. For each parameter the correction in a particular p_T bin is varied up and down within its statistical uncertainty to produce up and down templates. The total uncertainty in these corrections leads to an uncertainty in the signal templates of roughly 1%.

Pileup: to account for the uncertainty originating from the differences in the measured and simulated pileup distribution, the total inelastic cross section is varied by $\pm 4.6\%$ [81], and the reweighting factor applied to MC simulated samples is recomputed. Up and down MC simulation templates are constructed based on the up and down variations of the reweighting factor.

b tag veto efficiency: scale factors dependent on jet flavor, p_T , and η are applied to simulated events to correct for differences in b tagging efficiency and mistag rates between data and simulation [65]. Up and down templates are constructed based on the uncertainty in these efficiencies.

p_T^{miss} modeling: the uncertainty in the calibration of the jet energy scale and resolution affects the modeling of p_T^{miss} . These effects are estimated by changing the jet energy in the simulation up and down by one standard deviation. These up and down variations are used to construct sets of up and down templates for use in the fitting procedure.

As discussed in Section 2, there is also an uncertainty in the final measurement of A_{FB} based on the extrapolation from the fiducial region to the full phase space. This uncertainty is added as an additional source of systematic uncertainty when the correction is applied after the template fit.

The contributions from different sources of systematic uncertainty are evaluated by redoing the fit while different groups of nuisances are fixed to their nominal values and taking the quadrature difference between the resulting uncertainty and the full uncertainty. A comparison of the magnitude of the different systematic uncertainties on the A_{FB} and ΔA_{FB} measurements is shown in Table 1. The single largest source of systematic uncertainty in the measurement of A_{FB} are the PDFs, but it is a negligible source of uncertainty in the measurement of ΔA_{FB} . The dominant sources of systematic uncertainty are common to the electron and muon channels and thus their combination reduces the statistical uncertainty of the measurement but does not significantly reduce the systematic uncertainty.

9 Results

For all relevant results presented in this section, the best-fit value of the parameter and an approximate 68% CL confidence interval are extracted following the procedure described in Section 3.2 of [82]. The results for the template fits to data to extract A_{FB} in different mass bins are presented in Table 2 and shown graphically in Fig. 3; the results for A_0 are presented

Table 1: A comparison of the magnitude of the different sources of systematic uncertainty for the measurement of A_{FB} when combining the muon and electron channels and for the measurement of ΔA_{FB} . Results for the 170–200 GeV mass bin are shown because that is the mass bin in which the systematic uncertainty has the largest contribution to the total uncertainty; the results for other mass bins are similar. Results are also reported as a fraction of the overall systematic uncertainty for the measurement of A_{FB} and ΔA_{FB} . Sources are listed in order of the size of their contribution to the uncertainty in A_{FB} .

Source	Unc. on A_{FB} ($\times 10^{-3}$)	Frac. of total sys. unc. on A_{FB}	Unc. on ΔA_{FB} ($\times 10^{-3}$)	Frac. of total sys. unc. on ΔA_{FB}
PDFs	8.1	47%	0.8	1%
MC and MisID backgrounds stat. unc.	4.1	12%	6.8	42%
$\alpha_S + \mu_F/\mu_R$ scales	3.3	8%	3.2	9%
DY cross section	3.0	7%	0.9	1%
Pileup	2.8	5%	3.8	13%
Fiducial correction	2.7	5%	<0.1	<1%
t̄t cross section	2.7	5%	0.1	<1%
DY p_T correction	2.1	3%	0.8	1%
eμ shape corrections	1.8	2%	0.4	<1%
Integrated luminosity	1.2	1%	1.0	1%
Electron identification/isolation	1.0	1%	2.7	6%
Electron MisID normalization	0.9	1%	4.3	17%
Electron MisID shape	0.8	<1%	2.6	6%
b tagging uncertainty	0.8	<1%	0.3	<1%
p_T^{miss} uncertainties	0.7	<1%	0.5	<1%
Muon identification/isolation	0.6	<1%	1.2	1%
Muon MisID shape	0.5	<1%	0.6	<1%
$\gamma\gamma$ cross section	0.4	<1%	0.6	<1%
Muon MisID normalization	0.4	<1%	0.1	<1%
Electron trigger	0.4	<1%	1.2	1%
Diboson cross section	0.2	<1%	0.1	<1%
Electron reconstruction	0.2	<1%	0.7	<1%
Muon momentum scale	0.1	<1%	0.1	<1%
Electron momentum scale	0.1	<1%	0.1	<1%
Muon trigger	0.1	<1%	0.1	<1%

in Table 3 and shown graphically in Fig. 4. The results for the extraction of ΔA_{FB} and ΔA_0 in different mass bins and inclusively are presented in Table 4. The results for ΔA_{FB} are also shown graphically in Fig. 5. The resulting exclusion limits are shown in Fig. 6. The contribution of $\gamma\gamma \rightarrow \ell\ell$ events as compared to DY events in each mass bin is shown in Table 5. Comparisons of the data and the postfit predictions are shown in Figs. 7–9.

Table 2: Results for the measurement of A_{FB} from the maximum likelihood fit to data in different dilepton mass bins in the different channels as well as an inclusive measurement across all mass bins. The first and second uncertainties listed with each measurement are statistical and systematic, respectively. The last column lists the predictions of A_{FB} and associated uncertainties from aMC@NLO.

Mass (GeV)	A_{FB} muons	A_{FB} electrons	A_{FB} combined	aMC@NLO Pred.
170–200	$0.610 \pm 0.012 \pm 0.011$	$0.654 \pm 0.015 \pm 0.012$	$0.628 \pm 0.009 \pm 0.011$	0.612 ± 0.007
200–250	$0.592 \pm 0.012 \pm 0.010$	$0.635 \pm 0.015 \pm 0.011$	$0.608 \pm 0.009 \pm 0.010$	0.608 ± 0.006
250–320	$0.558 \pm 0.014 \pm 0.009$	$0.610 \pm 0.018 \pm 0.010$	$0.578 \pm 0.011 \pm 0.009$	0.603 ± 0.007
320–510	$0.598 \pm 0.014 \pm 0.009$	$0.583 \pm 0.018 \pm 0.009$	$0.592 \pm 0.011 \pm 0.008$	0.603 ± 0.005
510–700	$0.610 \pm 0.027 \pm 0.008$	$0.624 \pm 0.033 \pm 0.009$	$0.616 \pm 0.021 \pm 0.008$	0.604 ± 0.004
700–1000	$0.617 \pm 0.042 \pm 0.009$	$0.563 \pm 0.048 \pm 0.008$	$0.594 \pm 0.032 \pm 0.008$	0.606 ± 0.002
>1000	$0.595 \pm 0.070 \pm 0.011$	$0.694 \pm 0.076 \pm 0.014$	$0.638 \pm 0.052 \pm 0.011$	0.610 ± 0.002
Inclusive, Mass >170	$0.602 \pm 0.006 \pm 0.007$	$0.628 \pm 0.008 \pm 0.007$	$0.612 \pm 0.005 \pm 0.007$	0.608 ± 0.006

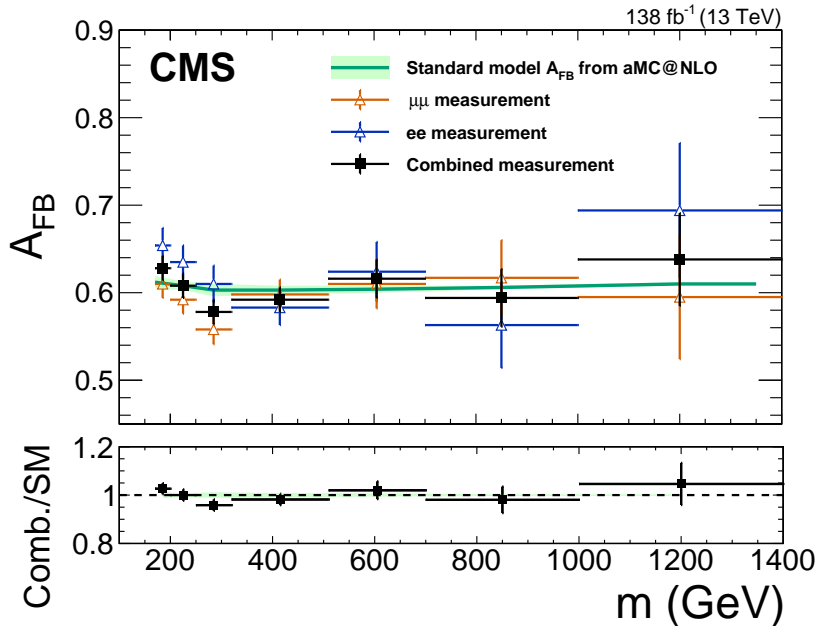


Figure 3: Measurement of the DY forward-backward asymmetry as a function the dilepton mass compared with the MC predictions. The green line is the predicted value for A_{FB} from the aMC@NLO simulation and the shaded green region its uncertainty. The red, blue, and black points and error bars represent the dimuon, dielectron, and combined measurements, respectively. Error bars on the measurements include both statistical and systematic components. The bottom panel shows the ratio between the combined measurement and the aMC@NLO prediction. In the bottom panel, the vertical error bars represent the uncertainty in the combined measurement and the shaded green band the uncertainty in the aMC@NLO prediction.

Table 3: Results for the measurement of A_0 from the maximum likelihood fit to data in different dilepton mass bins in the different channels as well as an inclusive measurement across all mass bins. The first and second uncertainties listed with each measurement are statistical and systematic, respectively. The last column lists the predictions of A_0 and associated uncertainties from aMC@NLO. To help in the interpretation of these results, we also list the average dilepton p_T of the data events in each mass bin.

Mass (GeV)	Avg. p_T (GeV)	A_0 muons	A_0 electrons	A_0 combined	aMC@NLO Pred.
170–200	38	$0.090 \pm 0.010 \pm 0.023$	$0.072 \pm 0.013 \pm 0.032$	$0.086 \pm 0.008 \pm 0.022$	0.06 ± 0.01
200–250	43	$0.041 \pm 0.011 \pm 0.024$	$0.069 \pm 0.015 \pm 0.050$	$0.045 \pm 0.009 \pm 0.024$	0.06 ± 0.01
250–320	48	$-0.027 \pm 0.016 \pm 0.029$	$0.065 \pm 0.021 \pm 0.044$	$-0.001 \pm 0.013 \pm 0.027$	0.06 ± 0.01
320–510	55	$-0.009 \pm 0.020 \pm 0.032$	$0.037 \pm 0.025 \pm 0.042$	$0.007 \pm 0.015 \pm 0.029$	0.05 ± 0.01
510–700	65	$-0.072 \pm 0.045 \pm 0.037$	$0.112 \pm 0.059 \pm 0.051$	$-0.005 \pm 0.036 \pm 0.034$	0.04 ± 0.01
700–1000	73	$0.053 \pm 0.081 \pm 0.039$	$0.086 \pm 0.099 \pm 0.068$	$0.065 \pm 0.063 \pm 0.040$	0.03 ± 0.01
>1000	88	$-0.251 \pm 0.140 \pm 0.048$	$-0.162 \pm 0.163 \pm 0.105$	$-0.219 \pm 0.107 \pm 0.050$	0.03 ± 0.01
Inclusive, Mass >170	44	$0.040 \pm 0.006 \pm 0.015$	$0.059 \pm 0.008 \pm 0.019$	$0.047 \pm 0.005 \pm 0.013$	0.06 ± 0.01

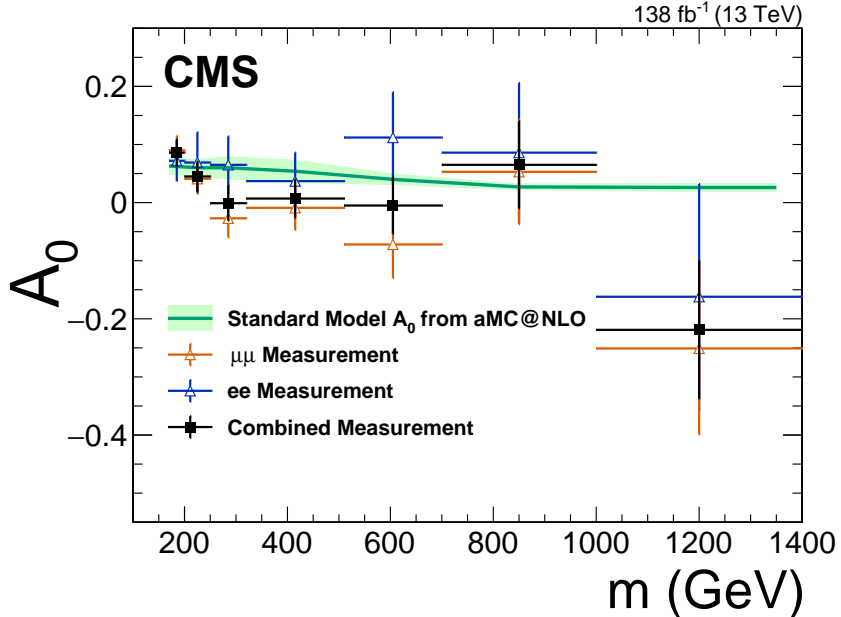


Figure 4: Measurement of the DY forward-backward asymmetry as a function the dilepton mass compared with the MC predictions. The green line is the predicted value for A_{FB} from the aMC@NLO simulation and the shaded green region its uncertainty. The red, blue, and black points and error bars represent the dimuon, dielectron, and combined measurements, respectively. Error bars on the measurements include both statistical and systematic components.

Table 4: Results for the measurement of ΔA_{FB} and ΔA_0 between the muon and electron channels from the maximum likelihood fit to data in different dilepton mass bins as well as an inclusive measurement across all mass bins. The first and second uncertainties listed with each measurement are statistical and systematic, respectively.

Mass (GeV)	ΔA_{FB}	ΔA_0
170–200	$-0.045 \pm 0.019 \pm 0.009$	$0.018 \pm 0.016 \pm 0.032$
200–250	$-0.042 \pm 0.019 \pm 0.006$	$-0.027 \pm 0.019 \pm 0.048$
250–320	$-0.052 \pm 0.023 \pm 0.006$	$-0.092 \pm 0.026 \pm 0.045$
320–510	$0.015 \pm 0.023 \pm 0.008$	$-0.046 \pm 0.032 \pm 0.045$
510–700	$-0.013 \pm 0.043 \pm 0.007$	$-0.184 \pm 0.075 \pm 0.053$
700–1000	$0.055 \pm 0.064 \pm 0.008$	$-0.034 \pm 0.128 \pm 0.068$
> 1000	$-0.099 \pm 0.104 \pm 0.014$	$-0.090 \pm 0.214 \pm 0.111$
Inclusive, Mass > 170	$-0.026 \pm 0.010 \pm 0.004$	$-0.018 \pm 0.011 \pm 0.018$

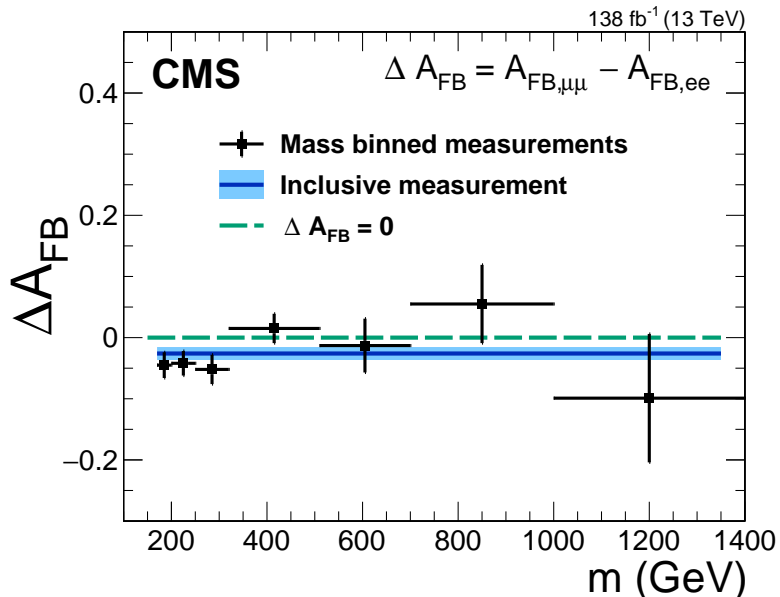


Figure 5: Measurement of the difference in forward-backward asymmetry between the dimuon and dielectron channels. The green line is drawn at zero, the predicted value for ΔA_{FB} assuming lepton flavor universality. The black points and error bars represent the measurements of ΔA_{FB} in different mass bins. The blue line and shaded light blue region represent the inclusive measurement of ΔA_{FB} and corresponding uncertainty. The error bars on the measurements and the shaded region include both statistical and systematic components.

Table 5: The fraction of photon-induced background as compared with the total amount of DY signal plus photon-induced events ($N_{\gamma\gamma}/(N_{\gamma\gamma} + N_{\text{DY}})$) in different dilepton mass bins. These numbers are averaged across the different years and channels.

Mass (GeV)	170–200	200–250	250–320	320–510	510–700	700–1000	> 1000
$\gamma\gamma \rightarrow \ell\ell$ fraction	1.8%	2.1%	2.5%	2.8%	3.3%	3.7%	4.1%

In the combined measurement of A_{FB} , no statistically significant deviations from the SM predictions are observed. A small difference is found between the muon and electron A_{FB} 's, with ΔA_{FB} found to be consistently below zero in the lowest three mass bins, as well as in the inclusive measurement. Based on a likelihood scan, the inclusive measurement ΔA_{FB} differs from zero at the level of 2.4 standard deviations.

Given that the existence of new gauge bosons would change the asymmetry well below their resonance masses, the measurement of A_{FB} can be used to constrain the existence of heavy Z' bosons. The constraining power is model dependent, because the interference between the Z' boson and Z/γ^* depends on the couplings of the Z' boson. To give an example of how these measurements can be used to constrain models with Z' bosons, constraints are derived for the sequential standard model (SSM) [83]. The SSM contains a Z' boson with the same coupling strength as the SM Z boson, up to an overall normalization factor in the left-handed coupling, κ_L . In order to set 95% confidence level (CL) upper limits on properties of the Z' boson, a hypothesis test between the SSM and SM is performed based on a comparison of the predicted values of A_{FB} in each model and our measurements. The test statistic used is the difference in χ^2 between the two models. Predictions for A_{FB} in the SSM Z' are derived from MC estimates using aMC@NLO [84]. Only the measurements of A_{FB} in the three highest mass bins are used for the χ^2 calculation. It was checked that the interference from an off-shell several- TeV SSM Z' produces negligible effects in the lower mass bins and their inclusion would not improve the limit.

Figure 6 shows the expected and observed 95% CL exclusion limits on SSM Z' bosons. For $\kappa_L = 1$, which corresponds to a Z' boson with exactly the same couplings as the SM Z boson, a Z' with $m_{Z'} < 4.4$ TeV is excluded at 95% CL, whereas the expected limit was 3.7 TeV.

Currently these limits are not as strong as those from direct dilepton resonance searches [21, 22], which report limits at 4.90 TeV and 5.15 by ATLAS and CMS, respectively. However, the A_{FB} -based approach is sensitive to wide-width resonances, which may be missed in a search for narrow resonances [7]. Additionally, the sensitivity of the A_{FB} -based approach will continue to improve with additional data, with the sensitivity to heavy mass scales expected to scale as the fourth root of the increase in integrated luminosity. This means limits from the A_{FB} -based approach should surpass the projected sensitivity of resonance searches [85] during the High-Luminosity upgrade of the LHC [86].

The full tabulated results are provided in HEPData [87].

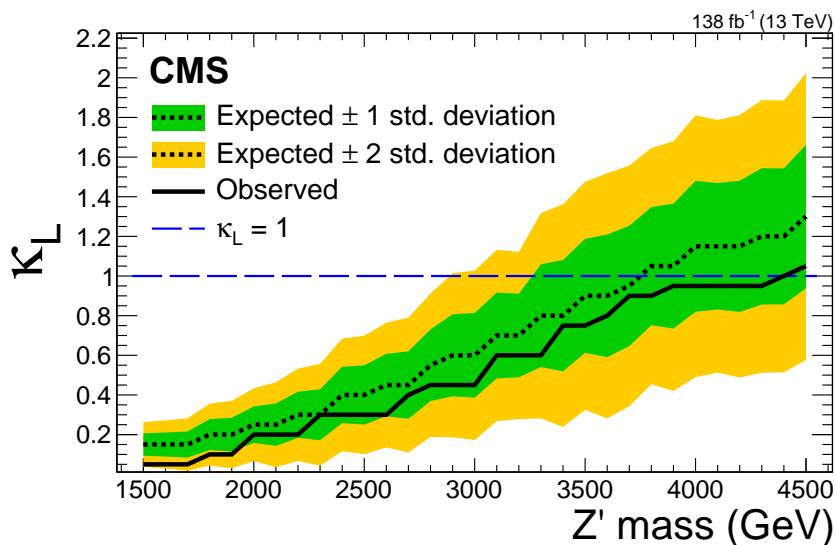


Figure 6: Exclusion limits at 95% CL on the coupling parameter κ_L for a Z' in the sequential standard model as a function of the Z' mass. The expected (observed) limit is shown by the dashed (solid) line. The inner and outer shaded areas around the expected limits show the 68% (green) and 95% (yellow) CL intervals, respectively. The dashed blue line shows $\kappa_L = 1$ which corresponds to a Z' with exactly the same couplings as the SM Z boson.

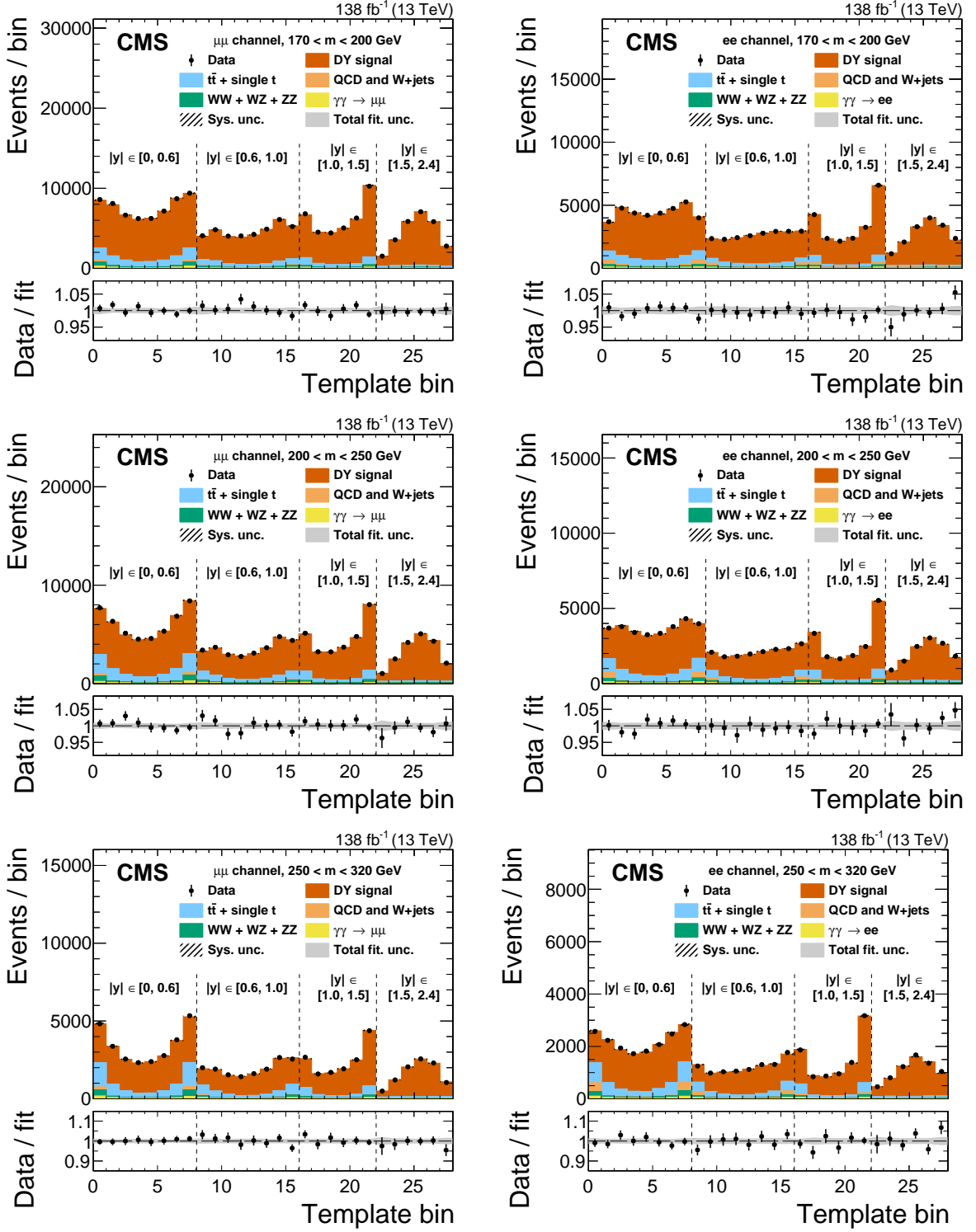


Figure 7: The postfit distributions in the 170–200, 200–250 and 250–320 GeV mass bins are shown in upper, middle and lower rows, respectively. The left column is the $\mu\mu$ channel, and the right column the ee channel. The contribution of the $\tau\tau$ background is not visible on the scale of these plots and has been omitted. The 2D templates follow the $\cos\theta_R$ and $|y|$ binning defined in Section 7 but are presented here in one dimension, with the dotted lines indicating the different $|y|$ bins. The black points and error bars represent the data and their statistical uncertainties. The bottom panel in each figure shows the ratio between the number of events observed in data and the best fit value. The gray shaded region in the bottom panel shows the total uncertainty in the best fit result.

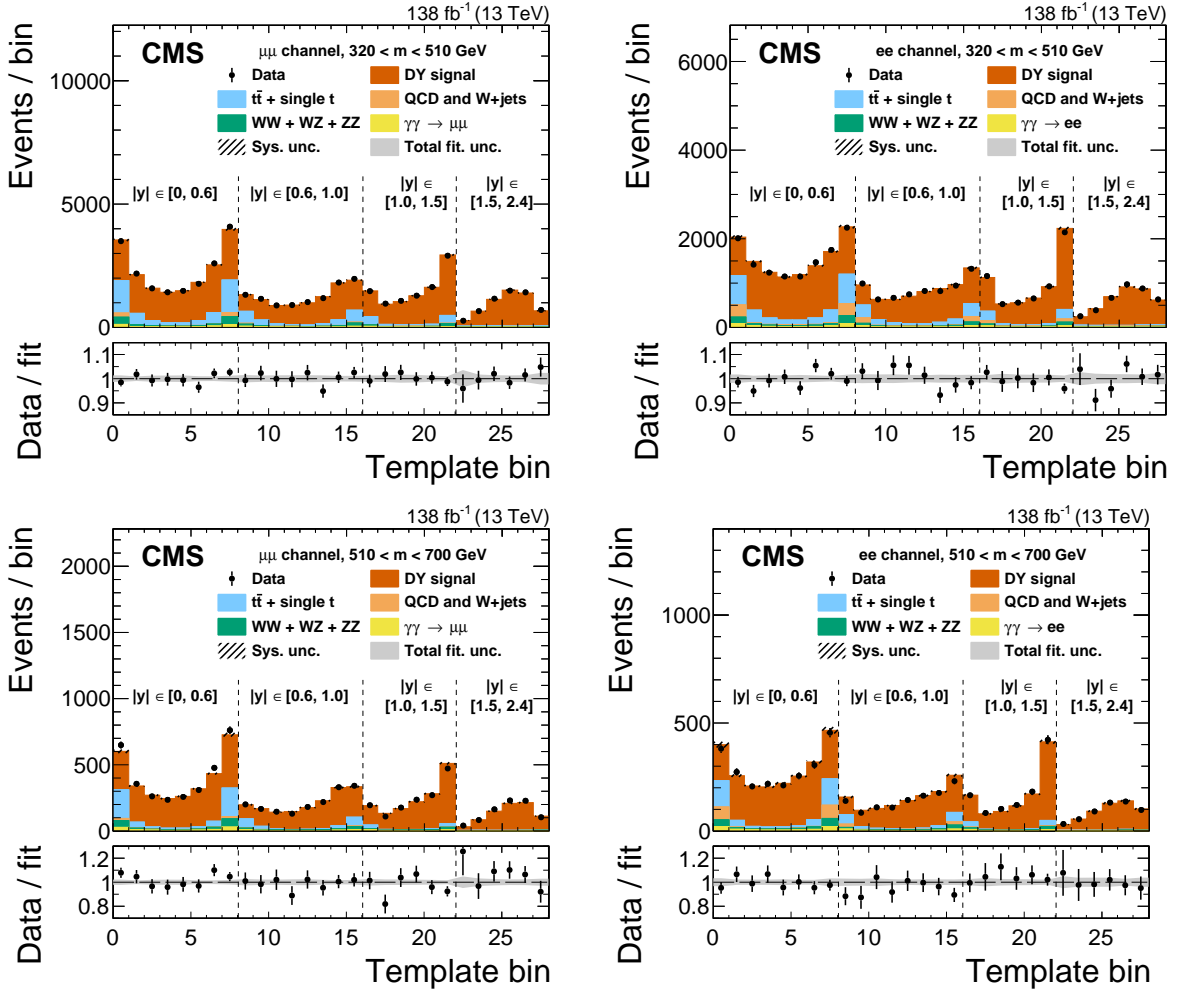


Figure 8: The postfit distributions in the 320 – 510 and 510 – 700 GeV mass bins are shown in the upper and lower rows, respectively. The left column is the $\mu\mu$ channel, and the right column the ee channel. The contribution of the $\tau\tau$ background is not visible on the scale of these plots and has been omitted. The 2D templates follow the $\cos\theta_R$ and $|y|$ binning defined in Section 7 but are presented here in one dimension, with the dotted lines indicating the different $|y|$ bins. The black points and error bars represent the data and their statistical uncertainties. The bottom panel in each figure shows the ratio between the number of events observed in data and the best fit value. The gray shaded region in the bottom panel shows the total uncertainty in the best fit result.

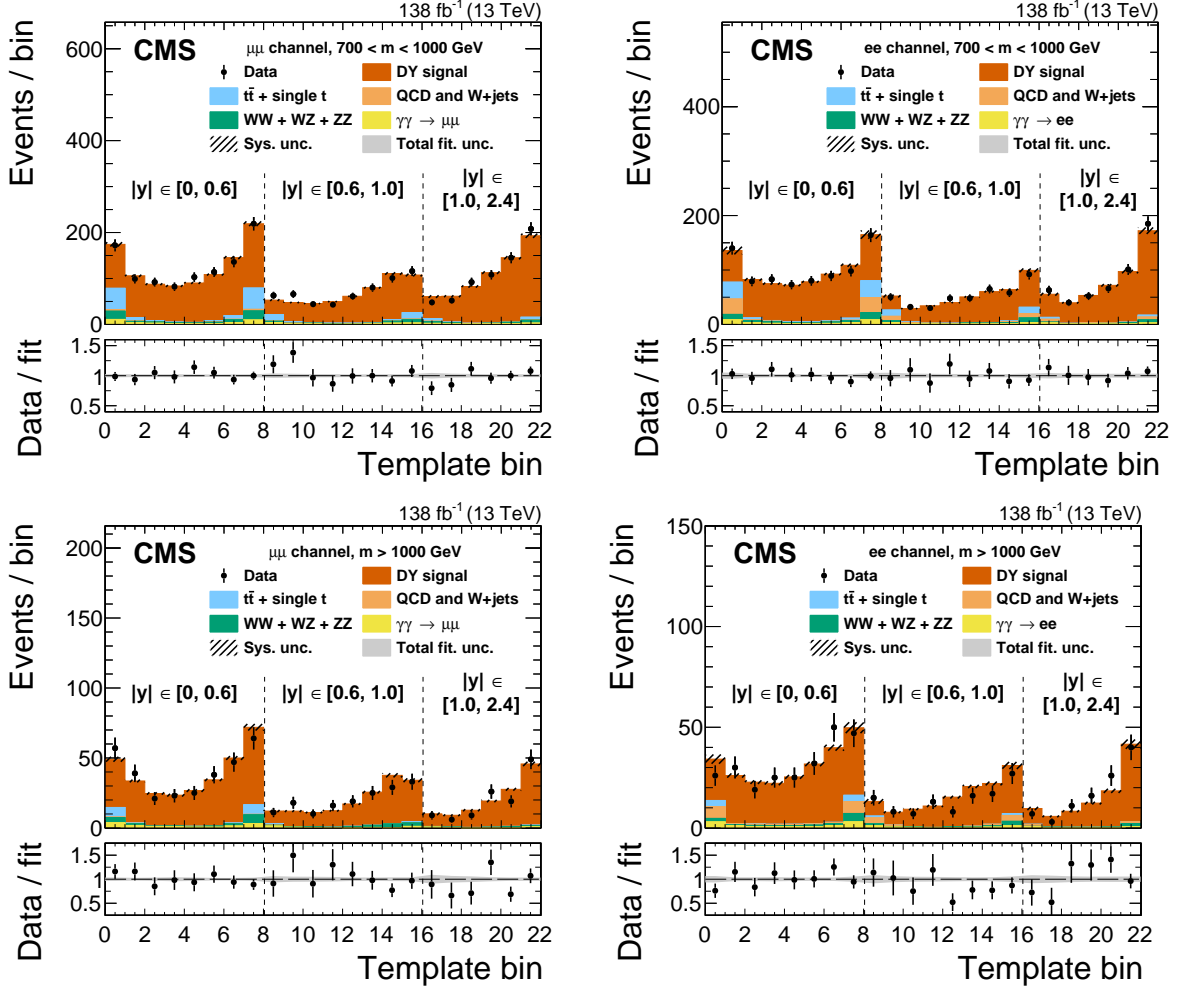


Figure 9: The postfit distributions in the 700–1000 and $>1000\text{ GeV}$ mass bins are shown in the upper and lower rows, respectively. The left plot is the $\mu\mu$ channel, and the right plot the ee channel. The contribution of the $\tau\tau$ background is not visible on the scale of these plots and has been omitted. The 2D templates follow the $\cos\theta_R$ and $|y|$ binning defined in Section 7 but are presented here in one dimension, with the dotted lines indicating the different $|y|$ bins. The black points and error bars represent the data and their statistical uncertainties. The bottom panel in each figure shows the ratio between the number of events observed in data and the best fit value. The gray shaded region in the bottom panel shows the total uncertainty in the best fit result.

10 Summary

The CMS detector at the LHC has been used to measure the Drell–Yan forward-backward asymmetry (A_{FB}) and the angular coefficient A_0 as functions of dilepton mass for muon and electron pairs with invariant mass above 170 GeV. The measurement is performed using proton-proton collision data collected in 2016–2018 at $\sqrt{s} = 13$ TeV with an integrated luminosity of 138 fb^{-1} using a template fitting approach. The combined dimuon and dielectron A_{FB} measurements show good agreement with the standard model predictions across the full mass range. An inclusive measurement across the full mass range yields an A_{FB} of $0.612 \pm 0.005 \text{ (stat)} \pm 0.007 \text{ (syst)}$ and an A_0 of $0.047 \pm 0.005 \text{ (stat)} \pm 0.013 \text{ (syst)}$. As a test of lepton flavor universality, the difference between the dimuon and dielectron A_{FB} s is measured and found to agree with zero to within 2.4 standard deviations. Using the combined A_{FB} measurements, limits are set on the existence of additional gauge bosons. For a Z' boson in the canonical sequential standard model the observed (expected) 95% confidence level lower limit on the Z' mass is 4.4 TeV (3.7 TeV).

Acknowledgments

We congratulate our colleagues in the CERN accelerator departments for the excellent performance of the LHC and thank the technical and administrative staffs at CERN and at other CMS institutes for their contributions to the success of the CMS effort. In addition, we gratefully acknowledge the computing centers and personnel of the Worldwide LHC Computing Grid and other centers for delivering so effectively the computing infrastructure essential to our analyses. Finally, we acknowledge the enduring support for the construction and operation of the LHC, the CMS detector, and the supporting computing infrastructure provided by the following funding agencies: BMBWF and FWF (Austria); FNRS and FWO (Belgium); CNPq, CAPES, FAPERJ, FAPERGS, and FAPESP (Brazil); MES (Bulgaria); CERN; CAS, MoST, and NSFC (China); MINCIENCIAS (Colombia); MSES and CSF (Croatia); RIF (Cyprus); SENESCYT (Ecuador); MoER, ERC PUT and ERDF (Estonia); Academy of Finland, MEC, and HIP (Finland); CEA and CNRS/IN2P3 (France); BMBF, DFG, and HGF (Germany); GSRT (Greece); NKFI (Hungary); DAE and DST (India); IPM (Iran); SFI (Ireland); INFN (Italy); MSIP and NRF (Republic of Korea); MES (Latvia); LAS (Lithuania); MOE and UM (Malaysia); BUAP, CINVESTAV, CONACYT, LNS, SEP, and UASLP-FAI (Mexico); MOS (Montenegro); MBIE (New Zealand); PAEC (Pakistan); MSHE and NSC (Poland); FCT (Portugal); JINR (Dubna); MON, RosAtom, RAS, RFBR, and NRC KI (Russia); MESTD (Serbia); SEIDI, CPAN, PCTI, and FEDER (Spain); MOSTR (Sri Lanka); Swiss Funding Agencies (Switzerland); MST (Taipei); ThEPCenter, IPST, STAR, and NSTDA (Thailand); TUBITAK and TAEK (Turkey); NASU (Ukraine); STFC (United Kingdom); DOE and NSF (USA).

Individuals have received support from the Marie-Curie program and the European Research Council and Horizon 2020 Grant, contract Nos. 675440, 724704, 752730, 765710 and 824093 (European Union); the Leventis Foundation; the Alfred P. Sloan Foundation; the Alexander von Humboldt Foundation; the Belgian Federal Science Policy Office; the Fonds pour la Formation à la Recherche dans l’Industrie et dans l’Agriculture (FRIA-Belgium); the Agentschap voor Innovatie door Wetenschap en Technologie (IWT-Belgium); the F.R.S.-FNRS and FWO (Belgium) under the “Excellence of Science – EOS” – be.h project n. 30820817; the Beijing Municipal Science & Technology Commission, No. Z191100007219010; the Ministry of Education, Youth and Sports (MEYS) of the Czech Republic; the Deutsche Forschungsgemeinschaft (DFG), under Germany’s Excellence Strategy – EXC 2121 “Quantum Universe” – 390833306, and under project number 400140256 - GRK2497; the Lendület (“Momentum”) Program and the János

Bolyai Research Scholarship of the Hungarian Academy of Sciences, the New National Excellence Program ÚNKP, the NKFIA research grants 123842, 123959, 124845, 124850, 125105, 128713, 128786, and 129058 (Hungary); the Council of Science and Industrial Research, India; the Latvian Council of Science; the Ministry of Science and Higher Education and the National Science Center, contracts Opus 2014/15/B/ST2/03998 and 2015/19/B/ST2/02861 (Poland); the National Priorities Research Program by Qatar National Research Fund; the Ministry of Science and Higher Education, project no. 0723-2020-0041 (Russia); the Programa Estatal de Fomento de la Investigación Científica y Técnica de Excelencia María de Maeztu, grant MDM-2015-0509 and the Programa Severo Ochoa del Principado de Asturias; the Thalis and Aristeia programs cofinanced by EU-ESF and the Greek NSRF; the Rachadapisek Sompot Fund for Postdoctoral Fellowship, Chulalongkorn University and the Chulalongkorn Academic into Its 2nd Century Project Advancement Project (Thailand); the Kavli Foundation; the Nvidia Corporation; the SuperMicro Corporation; the Welch Foundation, contract C-1845; and the Weston Havens Foundation (USA).

References

- [1] D. London and J. Rosner, "Extra gauge bosons in E_6 ", *Phys. Rev. D* **34** (1986) 1530, doi:10.1103/PhysRevD.34.1530.
- [2] J. Rosner, "Off-peak lepton asymmetries from new Z's", *Phys. Rev. D* **35** (1987) 2244, doi:10.1103/PhysRevD.35.2244.
- [3] J. Rosner, "Forward-backward asymmetries in hadronically produced lepton pairs", *Phys. Rev. D* **54** (1996) 1078, doi:10.1103/PhysRevD.54.1078, arXiv:hep-ph/9512299.
- [4] A. Bodek and U. Baur, "Implications of a 300-500 GeV/c^2 Z' boson on $p\bar{p}$ collider data at $\sqrt{s} = 1.8 \text{ TeV}$ ", *Eur. Phys. J. C* **21** (2001) 607, doi:10.1007/s100520100778, arXiv:hep-ph/0102160.
- [5] T. G. Rizzo, "Z' Phenomenology and the LHC", in *Theoretical Advanced Study Institute in Elementary Particle Physics: Exploring New Frontiers Using Colliders and Neutrinos*. 10, 2006. arXiv:hep-ph/0610104.
- [6] E. Accomando et al., "Forward-backward asymmetry as a discovery tool for Z' bosons at the LHC", *JHEP* **01** (2016) 127, doi:10.1007/JHEP01(2016)127, arXiv:1503.02672.
- [7] E. Accomando et al., "Production of Z'-boson resonances with large width at the LHC", *Phys. Lett. B* **803** (2020) 135293, doi:10.1016/j.physletb.2020.135293, arXiv:1910.13759.
- [8] E. Eichten, K. D. Lane, and M. E. Peskin, "New tests for quark and lepton substructure", *Phys. Rev. Lett.* **50** (1983) 811, doi:10.1103/PhysRevLett.50.811.
- [9] J. L. Hewett, "Indirect collider signals for extra dimensions", *Phys. Rev. Lett.* **82** (1999) 4765, doi:10.1103/PhysRevLett.82.4765, arXiv:hep-ph/9811356.
- [10] C. Gross, O. Lebedev, and J. M. No, "Drell-Yan constraints on new electroweak states: LHC as a $p p \rightarrow \ell^+ \ell^-$ precision machine", *Mod. Phys. Lett. A* **32** (2017) 1750094, doi:10.1142/S0217732317500948, arXiv:1602.03877.

- [11] R. M. Capdevilla, A. Delgado, A. Martin, and N. Raj, “Characterizing dark matter at the LHC in Drell-Yan events”, *Phys. Rev. D* **97** (2018) 035016, doi:10.1103/PhysRevD.97.035016, arXiv:1709.00439.
- [12] N. Raj, “Anticipating nonresonant new physics in dilepton angular spectra at the LHC”, *Phys. Rev. D* **95** (2017) 015011, doi:10.1103/PhysRevD.95.015011, arXiv:1610.03795.
- [13] LHCb Collaboration, “Test of lepton universality with $B^0 \rightarrow K^{*0} \ell^+ \ell^-$ decays”, *JHEP* **08** (2017) 055, doi:10.1007/JHEP08(2017)055, arXiv:1705.05802.
- [14] LHCb Collaboration, “Search for lepton-universality violation in $B^+ \rightarrow K^+ \ell^+ \ell^-$ decays”, *Phys. Rev. Lett.* **122** (2019) 191801, doi:10.1103/PhysRevLett.122.191801, arXiv:1903.09252.
- [15] LHCb Collaboration, “Test of lepton universality in beauty-quark decays”, 2021. arXiv:2103.11769.
- [16] B. C. Allanach, “ $U(1)_{B_3-L_2}$ explanation of the neutral current B -anomalies”, *Eur. Phys. J. C* **81** (2021) 56, doi:10.1140/epjc/s10052-021-08855-w, arXiv:2009.02197. [Erratum: doi:10.1140/epjc/s10052-021-09100-0].
- [17] D. Bećirević, N. Košnik, O. Sumensari, and R. Zukanovich Funchal, “Palatable leptoquark scenarios for lepton flavor violation in exclusive $b \rightarrow s\ell_1\ell_2$ modes”, *JHEP* **11** (2016) 035, doi:10.1007/JHEP11(2016)035, arXiv:1608.07583.
- [18] A. Greljo and D. Marzocca, “High- p_T dilepton tails and flavor physics”, *Eur. Phys. J. C* **77** (2017) 548, doi:10.1140/epjc/s10052-017-5119-8, arXiv:1704.09015.
- [19] E. Mirkes, “Angular decay distribution of leptons from W bosons at NLO in hadronic collisions”, *Nucl. Phys. B* **387** (1992) 3, doi:10.1016/0550-3213(92)90046-E.
- [20] E. Mirkes and J. Ohnemus, “Angular distributions of Drell-Yan lepton pairs at the Tevatron: Order $\alpha - s^2$ corrections and Monte Carlo studies”, *Phys. Rev. D* **51** (1995) 4891, doi:10.1103/PhysRevD.51.4891, arXiv:hep-ph/9412289.
- [21] ATLAS Collaboration, “Search for high-mass dilepton resonances using 139 fb^{-1} of pp collision data collected at $\sqrt{s} = 13 \text{ TeV}$ with the ATLAS detector”, *Phys. Lett. B* **796** (2019) 68, doi:10.1016/j.physletb.2019.07.016, arXiv:1903.06248.
- [22] CMS Collaboration, “Search for resonant and nonresonant new phenomena in high-mass dilepton final states at $\sqrt{s} = 13 \text{ TeV}$ ”, *JHEP* **07** (2021) 208, doi:10.1007/JHEP07(2021)208, arXiv:2103.02708.
- [23] J. Collins and D. Soper, “Angular distribution of dileptons in high-energy hadron collisions”, *Phys. Rev. D* **16** (1977) 2219, doi:10.1103/PhysRevD.16.2219.
- [24] CMS Collaboration, “Forward-backward asymmetry of Drell-Yan lepton pairs in pp collisions at $\sqrt{s} = 7 \text{ TeV}$ ”, *Phys. Lett. B* **718** (2013) 752, doi:10.1016/j.physletb.2012.10.082.
- [25] CMS Collaboration, “Forward-backward asymmetry of Drell-Yan lepton pairs in pp collisions at $\sqrt{s} = 8 \text{ TeV}$ ”, *Eur. Phys. J. C* **76** (2016) 325, doi:10.1140/epjc/s10052-016-4156-z.

- [26] ATLAS Collaboration, “Measurement of the forward-backward asymmetry of electron and muon pair-production in pp collisions at $\sqrt{s} = 7$ TeV with the ATLAS detector”, *JHEP* **09** (2015) 049, doi:10.1007/JHEP09(2015)049, arXiv:1503.03709.
- [27] CMS Collaboration, “Measurement of the weak mixing angle using the forward-backward asymmetry of Drell-Yan events in pp collisions at 8 TeV”, *Eur. Phys. J. C* **78** (2018) 701, doi:10.1140/epjc/s10052-018-6148-7, arXiv:1806.00863.
- [28] A. Bodek, “A simple event weighting technique for optimizing the measurement of the forward-backward asymmetry of Drell-Yan dilepton pairs at hadron colliders”, *Eur. Phys. J. C* **67** (2010) 321, doi:10.1140/epjc/s10052-010-1287-5, arXiv:0911.2850.
- [29] CMS Collaboration, “The CMS experiment at the CERN LHC”, *JINST* **3** (2008) S08004, doi:10.1088/1748-0221/3/08/S08004.
- [30] CMS Collaboration, “Performance of the CMS Level-1 trigger in proton-proton collisions at $\sqrt{s} = 13$ TeV”, *JINST* **15** (2020) P10017, doi:10.1088/1748-0221/15/10/P10017, arXiv:2006.10165.
- [31] CMS Collaboration, “The CMS trigger system”, *JINST* **12** (2017) P01020, doi:10.1088/1748-0221/12/01/P01020, arXiv:1609.02366.
- [32] CMS Collaboration, “Particle-flow reconstruction and global event description with the CMS detector”, *JINST* **12** (2017) P10003, doi:10.1088/1748-0221/12/10/P10003, arXiv:1706.04965.
- [33] M. Cacciari, G. P. Salam, and G. Soyez, “The anti- k_T jet clustering algorithm”, *JHEP* **04** (2008) 063, doi:10.1088/1126-6708/2008/04/063, arXiv:0802.1189.
- [34] M. Cacciari, G. P. Salam, and G. Soyez, “FastJet user manual”, *Eur. Phys. J. C* **72** (2012) 1896, doi:10.1140/epjc/s10052-012-1896-2, arXiv:1111.6097.
- [35] CMS Collaboration, “Performance of the CMS muon detector and muon reconstruction with proton-proton collisions at $\sqrt{s} = 13$ TeV”, *JINST* **13** (2018) P06015, doi:10.1088/1748-0221/13/06/P06015, arXiv:1804.04528.
- [36] CMS Collaboration, “Electron and photon reconstruction and identification with the CMS experiment at the CERN LHC”, *JINST* **16** (2021) P05014, doi:10.1088/1748-0221/16/05/P05014, arXiv:2012.06888.
- [37] CMS Collaboration, “Pileup mitigation at CMS in 13 TeV data”, *JINST* **15** (2020) P09018, doi:10.1088/1748-0221/15/09/p09018, arXiv:2003.00503.
- [38] CMS Collaboration, “Jet energy scale and resolution in the CMS experiment in pp collisions at 8 TeV”, *JINST* **12** (2017) P02014, doi:10.1088/1748-0221/12/02/P02014, arXiv:1607.03663.
- [39] CMS Collaboration, “Performance of missing transverse momentum reconstruction in proton-proton collisions at $\sqrt{s} = 13$ TeV using the CMS detector”, *JINST* **14** (2019) P07004, doi:10.1088/1748-0221/14/07/P07004, arXiv:1903.06078.
- [40] CMS Collaboration, “Precision luminosity measurement in proton-proton collisions at $\sqrt{s} = 13$ TeV in 2015 and 2016 at CMS”, *Eur. Phys. J. C* **81** (2021) 800, doi:10.1140/epjc/s10052-021-09538-2, arXiv:2104.01927.

- [41] CMS Collaboration, “CMS luminosity measurement for the 2017 data-taking period at $\sqrt{s} = 13$ TeV”, Physics Analysis Summary CMS-PAS-LUM-17-004, 2018.
- [42] CMS Collaboration, “CMS luminosity measurement for the 2018 data-taking period at $\sqrt{s} = 13$ TeV”, Physics Analysis Summary CMS-PAS-LUM-18-002, 2019.
- [43] J. Alwall et al., “The automated computation of tree-level and next-to-leading order differential cross sections, and their matching to parton shower simulations”, *JHEP* **07** (2014) 079, doi:10.1007/JHEP07(2014)079, arXiv:1405.0301.
- [44] R. Frederix and S. Frixione, “Merging meets matching in MC@NLO”, *JHEP* **12** (2012) 061, doi:10.1007/JHEP12(2012)061, arXiv:1209.6215.
- [45] T. Sjöstrand et al., “An introduction to PYTHIA 8.2”, *Comput. Phys. Commun.* **191** (2015) 159, doi:10.1016/j.cpc.2015.01.024, arXiv:1410.3012.
- [46] CMS Collaboration, “Event generator tunes obtained from underlying event and multiparton scattering measurements”, *Eur. Phys. J. C* **76** (2016) 155, doi:10.1140/epjc/s10052-016-3988-x, arXiv:1512.00815.
- [47] CMS Collaboration, “Extraction and validation of a new set of CMS PYTHIA8 tunes from underlying-event measurements”, *Eur. Phys. J. C* **80** (2020) 4, doi:10.1140/epjc/s10052-019-7499-4, arXiv:1903.12179.
- [48] R. D. Ball et al., “A first unbiased global NLO determination of parton distributions and their uncertainties”, *Nucl. Phys. B* **838** (2010) 136, doi:10.1016/j.nuclphysb.2010.05.008, arXiv:1002.4407.
- [49] NNPDF Collaboration, “Parton distributions for the LHC Run II”, *JHEP* **04** (2015) 040, doi:10.1007/JHEP04(2015)040, arXiv:1410.8849.
- [50] P. Nason, “A new method for combining NLO QCD with shower Monte Carlo algorithms”, *JHEP* **11** (2004) 040, doi:10.1088/1126-6708/2004/11/040, arXiv:hep-ph/0409146.
- [51] S. Frixione, P. Nason, and C. Oleari, “Matching NLO QCD computations with parton shower simulations: the POWHEG method”, *JHEP* **11** (2007) 070, doi:10.1088/1126-6708/2007/11/070, arXiv:0709.2092.
- [52] S. Alioli, P. Nason, C. Oleari, and E. Re, “A general framework for implementing NLO calculations in shower Monte Carlo programs: the POWHEG BOX”, *JHEP* **06** (2010) 043, doi:10.1007/JHEP06(2010)043, arXiv:1002.2581.
- [53] S. Frixione, P. Nason, and G. Ridolfi, “A positive-weight next-to-leading-order Monte Carlo for heavy flavour hadroproduction”, *JHEP* **09** (2007) 126, doi:10.1088/1126-6708/2007/09/126, arXiv:0707.3088.
- [54] CMS Collaboration, “Investigations of the impact of the parton shower tuning in Pythia 8 in the modelling of $t\bar{t}$ at $\sqrt{s} = 8$ and 13 TeV”, Physics Analysis Summary CMS-PAS-TOP-16-021, 2016.
- [55] L. Forthomme, “CepGen – A generic central exclusive processes event generator for hadron-hadron collisions”, *Comput. Phys. Commun.* **271** (2022) 108225, doi:10.1016/j.cpc.2021.108225, arXiv:1808.06059.

- [56] J. A. M. Vermaseren, “Two photon processes at very high-energies”, *Nucl. Phys. B* **229** (1983) 347, doi:10.1016/0550-3213(83)90336-X.
- [57] S. Baranov, O. Düenger, H. Shooshtari, and J. Vermaseren, “LPAIR: A generator for lepton pair production”, in *Workshop on Physics at HERA*, p. 1478. 1991.
- [58] T. Sjöstrand, S. Mrenna, and P. Z. Skands, “PYTHIA 6.4 physics and manual”, *JHEP* **05** (2006) 026, doi:10.1088/1126-6708/2006/05/026, arXiv:hep-ph/0603175.
- [59] A. Suri and D. R. Yennie, “The space-time phenomenology of photon absorbtion and inelastic electron scattering”, *Annals Phys.* **72** (1972) 243, doi:10.1016/0003-4916(72)90242-4.
- [60] J. M. Campbell, R. K. Ellis, and W. T. Giele, “A multi-threaded version of MCFM”, *Eur. Phys. J. C* **75** (2015) 246, doi:10.1140/epjc/s10052-015-3461-2, arXiv:1503.06182.
- [61] T. Gehrmann et al., “ W^+W^- production at hadron colliders in next to next to leading order QCD”, *Phys. Rev. Lett.* **113** (2014) 212001, doi:10.1103/PhysRevLett.113.212001, arXiv:1408.5243.
- [62] M. Czakon and A. Mitov, “Top++: A program for the calculation of the top-pair cross-section at hadron colliders”, *Comput. Phys. Commun.* **185** (2014) 2930, doi:10.1016/j.cpc.2014.06.021, arXiv:1112.5675.
- [63] GEANT4 Collaboration, “GEANT4—a simulation toolkit”, *Nucl. Instrum. Meth. A* **506** (2003) 250, doi:10.1016/S0168-9002(03)01368-8.
- [64] CMS Collaboration, “Performance of the reconstruction and identification of high-momentum muons in proton-proton collisions at $\sqrt{s} = 13$ TeV”, *JINST* **15** (2020) P02027, doi:10.1088/1748-0221/15/02/P02027, arXiv:1912.03516.
- [65] CMS Collaboration, “Identification of heavy-flavour jets with the CMS detector in pp collisions at 13 TeV”, *JINST* **13** (2018) P05011, doi:10.1088/1748-0221/13/05/P05011, arXiv:1712.07158.
- [66] CMS Collaboration, “Measurement of the differential Drell-Yan cross section in proton-proton collisions at $\sqrt{s} = 13$ TeV”, *JHEP* **12** (2019) 059, doi:10.1007/JHEP12(2019)059, arXiv:1812.10529.
- [67] CMS Collaboration, “Search for physics beyond the standard model in dilepton mass spectra in proton-proton collisions at $\sqrt{s} = 8$ TeV”, *JHEP* **04** (2015) 025, doi:10.1007/JHEP04(2015)025, arXiv:1412.6302.
- [68] Particle Data Group, P. A. Zyla et al., “Review of particle physics”, *Prog. Theor. Exp. Phys.* **2020** (2020) 083C01, doi:10.1093/ptep/ptaa104.
- [69] CMS Collaboration, “Measurement of the top quark forward-backward production asymmetry and the anomalous chromoelectric and chromomagnetic moments in pp collisions at $\sqrt{s} = 13$ TeV”, *JHEP* **06** (2020) 146, doi:10.1007/JHEP06(2020)146, arXiv:1912.09540.
- [70] S. Carrazza et al., “An unbiased Hessian representation for Monte Carlo PDFs”, *Eur. Phys. J. C* **75** (2015) 369, doi:10.1140/epjc/s10052-015-3590-7, arXiv:1505.06736.

- [71] A. Bodek et al., “Extracting muon momentum scale corrections for hadron collider experiments”, *Eur. Phys. J. C* **72** (2012) 2194,
`doi:10.1140/epjc/s10052-012-2194-8`, [arXiv:1208.3710](#).
- [72] R. Gavin, Y. Li, F. Petriello, and S. Quackenbush, “FEWZ 2.0: A code for hadronic Z production at next-to-next-to-leading order”, *Comput. Phys. Commun.* **182** (2011) 2388,
`doi:10.1016/j.cpc.2011.06.008`, [arXiv:1011.3540](#).
- [73] F. Cascioli et al., “ZZ production at hadron colliders in NNLO QCD”, *Phys. Lett. B* **735** (2014) 311, `doi:10.1016/j.physletb.2014.06.056`, [arXiv:1405.2219](#).
- [74] J. M. Campbell, R. K. Ellis, and C. Williams, “Vector boson pair production at the LHC”, *JHEP* **07** (2011) 018, `doi:10.1007/JHEP07(2011)018`, [arXiv:1105.0020](#).
- [75] A. Manohar, P. Nason, G. P. Salam, and G. Zanderighi, “How bright is the proton? A precise determination of the photon parton distribution function”, *Phys. Rev. Lett.* **117** (2016) 242002, `doi:10.1103/PhysRevLett.117.242002`, [arXiv:1607.04266](#).
- [76] A. V. Manohar, P. Nason, G. P. Salam, and G. Zanderighi, “The photon content of the proton”, *JHEP* **12** (2017) 046, `doi:10.1007/JHEP12(2017)046`, [arXiv:1708.01256](#).
- [77] J. S. Conway, “Incorporating nuisance parameters in likelihoods for multisource spectra”, in *Proceedings, PHYSTAT 2011 Workshop on Statistical Issues Related to Discovery Claims in Search Experiments and Unfolding*, p. 115. 2011. [arXiv:1103.0354](#). CERN, Geneva, Switzerland, 17–20 Jan. 2011. `doi:10.5170/CERN-2011-006.115`.
- [78] J. Butterworth et al., “PDF4LHC recommendations for LHC Run II”, *J. Phys. G* **43** (2016) 023001, `doi:10.1088/0954-3899/43/2/023001`, [arXiv:1510.03865](#).
- [79] ATLAS Collaboration, “Measurement of the transverse momentum distribution of Drell–Yan lepton pairs in proton–proton collisions at $\sqrt{s} = 13$ TeV with the ATLAS detector”, *Eur. Phys. J. C* **80** (2020) 616, `doi:10.1140/epjc/s10052-020-8001-z`, [arXiv:1912.02844](#).
- [80] CMS Collaboration, “Measurements of differential Z boson production cross sections in proton–proton collisions at $\sqrt{s} = 13$ TeV”, *JHEP* **12** (2019) 061, `doi:10.1007/JHEP12(2019)061`, [arXiv:1909.04133](#).
- [81] CMS Collaboration, “Measurement of the inelastic proton–proton cross section at $\sqrt{s} = 13$ TeV”, *JHEP* **07** (2018) 161, `doi:10.1007/JHEP07(2018)161`, [arXiv:1802.02613](#).
- [82] CMS Collaboration, “Precise determination of the mass of the Higgs boson and tests of compatibility of its couplings with the standard model predictions using proton collisions at 7 and 8 TeV”, *Eur. Phys. J. C* **75** (2015) 212, `doi:10.1140/epjc/s10052-015-3351-7`, [arXiv:1412.8662](#).
- [83] G. Altarelli, B. Mele, and M. Ruiz-Altaba, “Searching for new heavy vector bosons in p \bar{p} colliders”, *Z. Phys. C* **45** (1989) 109, `doi:10.1007/BF01556677`. [Erratum:
`doi:10.1007/BF01552335`].
- [84] B. Fuks and R. Ruiz, “A comprehensive framework for studying W' and Z' bosons at hadron colliders with automated jet veto resummation”, *JHEP* **05** (2017) 032, `doi:10.1007/JHEP05(2017)032`, [arXiv:1701.05263](#).

- [85] X. Cid Vidal et al., “Report from working group 3: Beyond the standard model physics at the HL-LHC and HE-LHC”, CERN Report CERN-LPCC-2018-05, 2019.
doi:10.23731/CYRM-2019-007.585, arXiv:1812.07831.
- [86] I. Zurbano Fernandez et al., “High-Luminosity Large Hadron Collider (HL-LHC): technical design report”, CERN Report CERN-2020-010, 12, 2020.
doi:10.23731/CYRM-2020-0010.
- [87] HEPData record for this analysis, 2022. *doi*:10.17182/hepdata.114012.

A The CMS Collaboration

Yerevan Physics Institute, Yerevan, Armenia

A. Tumasyan

Institut für Hochenergiephysik, Vienna, Austria

W. Adam , J.W. Andrejkovic, T. Bergauer , S. Chatterjee , K. Damanakis, M. Dragicevic , A. Escalante Del Valle , R. Frühwirth¹, M. Jeitler¹ , N. Krammer, L. Lechner , D. Liko, I. Mikulec, P. Paulitsch, F.M. Pitters, J. Schieck¹ , R. Schöfbeck , D. Schwarz, S. Templ , W. Waltenberger , C.-E. Wulz¹ 

Institute for Nuclear Problems, Minsk, Belarus

V. Makarenko , T. Nechaeva, U. Yevarouskaya

Universiteit Antwerpen, Antwerpen, Belgium

M.R. Darwish², E.A. De Wolf, T. Janssen , T. Kello³, A. Lelek , H. Rejeb Sfar, P. Van Mechelen , S. Van Putte, N. Van Remortel 

Vrije Universiteit Brussel, Brussel, Belgium

E.S. Bols , J. D'Hondt , A. De Moor, M. Delcourt, H. El Faham , S. Lowette , S. Moortgat , A. Morton , D. Müller , A.R. Sahasransu , S. Tavernier , W. Van Doninck, D. Vannerom 

Université Libre de Bruxelles, Bruxelles, Belgium

D. Beghin, B. Bilin , B. Clerbaux , G. De Lentdecker, L. Favart , A.K. Kalsi , K. Lee, M. Mahdavikhorrami, I. Makarenko , L. Moureaux , S. Paredes , L. Pétré, A. Popov , N. Postiau, E. Starling , L. Thomas , M. Vanden Bemden, C. Vander Velde , P. Vanlaer 

Ghent University, Ghent, Belgium

T. Cornelis , D. Dobur, J. Knolle , L. Lambrecht, G. Mestdach, M. Niedziela , C. Rendón, C. Roskas, A. Samalan, K. Skovpen , M. Tytgat , B. Vermassen, L. Wezenbeek

Université Catholique de Louvain, Louvain-la-Neuve, Belgium

A. Benecke, A. Bethani , G. Bruno, F. Bury , C. Caputo , P. David , C. Delaere , I.S. Donertas , A. Giannanco , K. Jaffel, Sa. Jain , V. Lemaitre, K. Mondal , J. Prisciandaro, A. Taliercio, M. Teklishyn , T.T. Tran, P. Vischia , S. Wertz 

Centro Brasileiro de Pesquisas Fisicas, Rio de Janeiro, Brazil

G.A. Alves , C. Hensel, A. Moraes , P. Rebello Teles 

Universidade do Estado do Rio de Janeiro, Rio de Janeiro, Brazil

W.L. Aldá Júnior , M. Alves Gallo Pereira , M. Barroso Ferreira Filho, H. Brandao Malbouisson, W. Carvalho , J. Chinellato⁴, E.M. Da Costa , G.G. Da Silveira⁵ , D. De Jesus Damiao , V. Dos Santos Sousa, S. Fonseca De Souza , C. Mora Herrera , K. Mota Amarilo, L. Mundim , H. Nogima, A. Santoro, S.M. Silva Do Amaral , A. Sznajder , M. Thiel, F. Torres Da Silva De Araujo⁶ , A. Vilela Pereira 

Universidade Estadual Paulista (a), Universidade Federal do ABC (b), São Paulo, Brazil

C.A. Bernardes⁵ , L. Calligaris , T.R. Fernandez Perez Tomei , E.M. Gregores , D.S. Lemos , P.G. Mercadante , S.F. Novaes , Sandra S. Padula 

Institute for Nuclear Research and Nuclear Energy, Bulgarian Academy of Sciences, Sofia, Bulgaria

A. Aleksandrov, G. Antchev , R. Hadjiiska, P. Iaydjiev, M. Misheva, M. Rodozov, M. Shopova, G. Sultanov

University of Sofia, Sofia, Bulgaria

A. Dimitrov, T. Ivanov, L. Litov , B. Pavlov, P. Petkov, A. Petrov

Beihang University, Beijing, China

T. Cheng , T. Javaid⁷, M. Mittal, L. Yuan

Department of Physics, Tsinghua University, Beijing, China

M. Ahmad , G. Bauer, C. Dozen⁸ , Z. Hu , J. Martins⁹ , Y. Wang, K. Yi^{10,11}

Institute of High Energy Physics, Beijing, China

E. Chapon , G.M. Chen⁷ , H.S. Chen⁷ , M. Chen , F. Iemmi, A. Kapoor , D. Leggat, H. Liao, Z.-A. Liu⁷ , V. Milosevic , F. Monti , R. Sharma , J. Tao , J. Thomas-Wilsker, J. Wang , H. Zhang , J. Zhao 

State Key Laboratory of Nuclear Physics and Technology, Peking University, Beijing, China

A. Agapitos, Y. An, Y. Ban, C. Chen, A. Levin , Q. Li , X. Lyu, Y. Mao, S.J. Qian, D. Wang , J. Xiao, H. Yang

Sun Yat-Sen University, Guangzhou, China

M. Lu, Z. You 

Institute of Modern Physics and Key Laboratory of Nuclear Physics and Ion-beam Application (MOE) - Fudan University, Shanghai, China

X. Gao³, H. Okawa , Y. Zhang 

Zhejiang University, Hangzhou, China, Zhejiang, China

Z. Lin , M. Xiao 

Universidad de Los Andes, Bogota, Colombia

C. Avila , A. Cabrera , C. Florez , J. Fraga

Universidad de Antioquia, Medellin, Colombia

J. Mejia Guisao, F. Ramirez, J.D. Ruiz Alvarez 

University of Split, Faculty of Electrical Engineering, Mechanical Engineering and Naval Architecture, Split, Croatia

D. Giljanovic, N. Godinovic , D. Lelas , I. Puljak 

University of Split, Faculty of Science, Split, Croatia

Z. Antunovic, M. Kovac, T. Sculac 

Institute Rudjer Boskovic, Zagreb, Croatia

V. Brigljevic , D. Ferencek , D. Majumder , M. Roguljic, A. Starodumov¹² , T. Susa 

University of Cyprus, Nicosia, Cyprus

A. Attikis , K. Christoforou, A. Ioannou, G. Kole , M. Kolosova, S. Konstantinou, J. Mousa , C. Nicolaou, F. Ptochos , P.A. Razis, H. Rykaczewski, H. Saka 

Charles University, Prague, Czech Republic

M. Finger¹³, M. Finger Jr.¹³ , A. Kveton

Escuela Politecnica Nacional, Quito, Ecuador

E. Ayala

Universidad San Francisco de Quito, Quito, Ecuador

E. Carrera Jarrin 

Academy of Scientific Research and Technology of the Arab Republic of Egypt, Egyp-

tian Network of High Energy Physics, Cairo, Egypt

A.A. Abdelalim^{14,15} , Y. Assran^{16,17}

Center for High Energy Physics (CHEP-FU), Fayoum University, El-Fayoum, Egypt

M.A. Mahmoud , Y. Mohammed 

National Institute of Chemical Physics and Biophysics, Tallinn, Estonia

S. Bhowmik , R.K. Dewanjee , K. Ehataht, M. Kadastik, S. Nandan, C. Nielsen, J. Pata, M. Raidal , L. Tani, C. Veelken

Department of Physics, University of Helsinki, Helsinki, Finland

P. Eerola , H. Kirschenmann , K. Osterberg , M. Voutilainen 

Helsinki Institute of Physics, Helsinki, Finland

S. Barthuar, E. Brücken , F. Garcia , J. Havukainen , M.S. Kim , R. Kinnunen, T. Lampén, K. Lassila-Perini , S. Lehti , T. Lindén, M. Lotti, L. Martikainen, M. Myllymäki, J. Ott , H. Siikonen, E. Tuominen , J. Tuominiemi

Lappeenranta University of Technology, Lappeenranta, Finland

P. Luukka , H. Petrow, T. Tuuva

IRFU, CEA, Université Paris-Saclay, Gif-sur-Yvette, France

C. Amendola , M. Besancon, F. Couderc , M. Dejardin, D. Denegri, J.L. Faure, F. Ferri , S. Ganjour, P. Gras, G. Hamel de Monchenault , P. Jarry, B. Lenzi , E. Locci, J. Malcles, J. Rander, A. Rosowsky , M.Ö. Sahin , A. Savoy-Navarro¹⁸, M. Titov , G.B. Yu 

Laboratoire Leprince-Ringuet, CNRS/IN2P3, Ecole Polytechnique, Institut Polytechnique de Paris, Palaiseau, France

S. Ahuja , F. Beaudette , M. Bonanomi , A. Buchot Perraguin, P. Busson, A. Cappati, C. Charlot, O. Davignon, B. Diab, G. Falmagne , S. Ghosh, R. Granier de Cassagnac , A. Hakimi, I. Kucher , J. Motta, M. Nguyen , C. Ochando , P. Paganini , J. Rembser, R. Salerno , U. Sarkar , J.B. Sauvan , Y. Sirois , A. Tarabini, A. Zabi, A. Zghiche 

Université de Strasbourg, CNRS, IPHC UMR 7178, Strasbourg, France

J.-L. Agram¹⁹ , J. Andrea, D. Apparu, D. Bloch , G. Bourgatte, J.-M. Brom, E.C. Chabert, C. Collard , D. Darej, J.-C. Fontaine¹⁹, U. Goerlach, C. Grimault, A.-C. Le Bihan, E. Nibigira , P. Van Hove 

Institut de Physique des 2 Infinis de Lyon (IP2I), Villeurbanne, France

E. Asilar , S. Beauceron , C. Bernet , G. Boudoul, C. Camen, A. Carle, N. Chanon , D. Contardo, P. Depasse , H. El Mamouni, J. Fay, S. Gascon , M. Gouzevitch , B. Ille, I.B. Laktineh, H. Lattaud , A. Lesauvage , M. Lethuillier , L. Mirabito, S. Perries, K. Shchablo, V. Sordini , L. Torterotot , G. Touquet, M. Vander Donckt, S. Viret

Georgian Technical University, Tbilisi, Georgia

I. Lomidze, T. Toriashvili²⁰, Z. Tsamalaidze¹³

RWTH Aachen University, I. Physikalisches Institut, Aachen, Germany

V. Botta, L. Feld , K. Klein, M. Lipinski, D. Meuser, A. Pauls, N. Röwert, J. Schulz, M. Teroerde 

RWTH Aachen University, III. Physikalisches Institut A, Aachen, Germany

A. Dodonova, D. Eliseev, M. Erdmann , P. Fackeldey , B. Fischer, T. Hebbeker , K. Hoepfner, F. Ivone, L. Mastrolorenzo, M. Merschmeyer , A. Meyer , G. Mocellin, S. Mondal, S. Mukherjee , D. Noll , A. Novak, A. Pozdnyakov , Y. Rath, H. Reithler,

A. Schmidt , S.C. Schuler, A. Sharma , L. Vigilante, S. Wiedenbeck, S. Zaleski

RWTH Aachen University, III. Physikalisches Institut B, Aachen, Germany

C. Dziwok, G. Flügge, W. Haj Ahmad²¹ , O. Hlushchenko, T. Kress, A. Nowack , O. Pooth, D. Roy , A. Stahl²² , T. Ziemons , A. Zotz

Deutsches Elektronen-Synchrotron, Hamburg, Germany

H. Aarup Petersen, M. Aldaya Martin, P. Asmuss, S. Baxter, M. Bayatmakou, O. Behnke, A. Bermúdez Martínez, S. Bhattacharya, A.A. Bin Anuar , F. Blekman , K. Borras²³, D. Brunner, A. Campbell , A. Cardini , C. Cheng, F. Colombina, S. Consuegra Rodríguez , G. Correia Silva, V. Danilov, M. De Silva, L. Didukh, G. Eckerlin, D. Eckstein, L.I. Estevez Banos , O. Filatov , E. Gallo²⁴, A. Geiser, A. Giraldi, A. Grohsjean , M. Guthoff, A. Jafari²⁵ , N.Z. Jomhari , H. Jung , A. Kasem²³ , M. Kasemann , H. Kaveh , C. Kleinwort , R. Kogler , D. Krücker , W. Lange, K. Lipka, W. Lohmann²⁶, R. Mankel, I.-A. Melzer-Pellmann , M. Mendizabal Morentin, J. Metwally, A.B. Meyer , M. Meyer , J. Mnich , A. Mussgiller, A. Nürnberg, Y. Otarid, D. Pérez Adán , D. Pitzl, A. Raspereza, B. Ribeiro Lopes, J. Rübenach, A. Saggio , A. Saibel , M. Savitskyi , M. Scham²⁷, V. Scheurer, S. Schnake, P. Schütze, C. Schwanenberger²⁴ , M. Shchedrolosiev, R.E. Sosa Ricardo , D. Stafford, N. Tonon , M. Van De Klundert , F. Vazzoler , R. Walsh , D. Walter, Q. Wang , Y. Wen , K. Wichmann, L. Wiens, C. Wissing, S. Wuchterl 

University of Hamburg, Hamburg, Germany

R. Aggleton, S. Albrecht , S. Bein , L. Benato , P. Connor , K. De Leo , M. Eich, K. El Morabit, F. Feindt, A. Fröhlich, C. Garbers , E. Garutti , P. Gunnellini, M. Hajheidari, J. Haller , A. Hinzmann , G. Kasieczka, R. Klanner , T. Kramer, V. Kutzner, J. Lange , T. Lange , A. Lobanov , A. Malara , A. Mehta , A. Nigamova, K.J. Pena Rodriguez, M. Rieger , O. Rieger, P. Schleper, M. Schröder , J. Schwandt , J. Sonneveld , H. Stadie, G. Steinbrück, A. Tews, I. Zoi 

Karlsruher Institut fuer Technologie, Karlsruhe, Germany

J. Bechtel , S. Brommer, M. Burkart, E. Butz , R. Caspart , T. Chwalek, W. De Boer[†], A. Dierlamm, A. Droll, N. Faltermann , M. Giffels, J.O. Gosewisch, A. Gottmann, F. Hartmann²² , C. Heidecker, U. Husemann , P. Keicher, R. Koppenhöfer, S. Maier, M. Metzler, S. Mitra , Th. Müller, M. Neukum, G. Quast , K. Rabbertz , J. Rauser, D. Savoiu , M. Schnepf, D. Seith, I. Shvetsov, H.J. Simonis, R. Ulrich , J. Van Der Linden, R.F. Von Cube, M. Wassmer, M. Weber , S. Wieland, R. Wolf , S. Wozniewski, S. Wunsch

Institute of Nuclear and Particle Physics (INPP), NCSR Demokritos, Aghia Paraskevi, Greece

G. Anagnostou, G. Daskalakis, A. Kyriakis, D. Loukas, A. Stakia 

National and Kapodistrian University of Athens, Athens, Greece

M. Diamantopoulou, D. Karasavvas, P. Kontaxakis , C.K. Koraka, A. Manousakis-Katsikakis, A. Panagiotou, I. Papavergou, N. Saoulidou , K. Theofilatos , E. Tziaferi , K. Vellidis, E. Vourliotis

National Technical University of Athens, Athens, Greece

G. Bakas, K. Kousouris , I. Papakrivopoulos, G. Tsipolitis, A. Zacharopoulou

University of Ioánnina, Ioánnina, Greece

K. Adamidis, I. Bestintzanos, I. Evangelou , C. Foudas, P. Gianneios, P. Katsoulis, P. Kokkas, N. Manthos, I. Papadopoulos , J. Strologas 

MTA-ELTE Lendület CMS Particle and Nuclear Physics Group, Eötvös Loránd University, Budapest, Hungary

M. Csanad , K. Farkas, M.M.A. Gadallah²⁸ , S. Lököс²⁹ , P. Major, K. Mandal , G. Pasztor , A.J. Rádl, O. Surányi, G.I. Veres 

Wigner Research Centre for Physics, Budapest, Hungary

M. Bartók³⁰ , G. Bencze, C. Hajdu , D. Horvath^{31,32} , F. Sikler , V. Veszpremi 

Institute of Nuclear Research ATOMKI, Debrecen, Hungary

S. Czellar, D. Fasanella , F. Fienga , J. Karancsi³⁰ , J. Molnar, Z. Szillasi, D. Teyssier

Institute of Physics, University of Debrecen, Debrecen, Hungary

P. Raics, Z.L. Trocsanyi³³ , B. Ujvari³⁴

Karoly Robert Campus, MATE Institute of Technology, Gyongyos, Hungary

T. Csorgo³⁵ , F. Nemes³⁵, T. Novak

National Institute of Science Education and Research, HBNI, Bhubaneswar, India

S. Bahinipati³⁶ , C. Kar , P. Mal, T. Mishra , V.K. Muraleedharan Nair Bindhu³⁷, A. Nayak³⁷ , P. Saha, N. Sur , S.K. Swain, D. Vats³⁷

Panjab University, Chandigarh, India

S. Bansal , S.B. Beri, V. Bhatnagar , G. Chaudhary , S. Chauhan , N. Dhingra³⁸ , R. Gupta, A. Kaur, H. Kaur, M. Kaur , P. Kumari , M. Meena, K. Sandeep , J.B. Singh³⁹ , A.K. Virdi 

University of Delhi, Delhi, India

A. Ahmed, A. Bhardwaj , B.C. Choudhary , M. Gola, S. Keshri , A. Kumar , M. Naimuddin , P. Priyanka , K. Ranjan, A. Shah 

Saha Institute of Nuclear Physics, HBNI, Kolkata, India

M. Bharti⁴⁰, R. Bhattacharya, S. Bhattacharya , D. Bhowmik, S. Dutta, S. Dutta, B. Gomber⁴¹ , M. Maity⁴², P. Palit , P.K. Rout , G. Saha, B. Sahu , S. Sarkar, M. Sharan

Indian Institute of Technology Madras, Madras, India

P.K. Behera , S.C. Behera, P. Kalbhor , J.R. Komaragiri⁴³ , D. Kumar⁴³, A. Muhammad, L. Panwar⁴³ , R. Pradhan, P.R. Pujahari, A. Sharma , A.K. Sikdar, P.C. Tiwari⁴³ 

Bhabha Atomic Research Centre, Mumbai, India

K. Naskar⁴⁴

Tata Institute of Fundamental Research-A, Mumbai, India

T. Aziz, S. Dugad, M. Kumar, G.B. Mohanty 

Tata Institute of Fundamental Research-B, Mumbai, India

S. Banerjee , R. Chudasama, M. Guchait, S. Karmakar, S. Kumar, G. Majumder, K. Mazumdar, S. Mukherjee 

Indian Institute of Science Education and Research (IISER), Pune, India

A. Alpana, S. Dube , B. Kansal, A. Laha, S. Pandey , A. Rastogi , S. Sharma 

Isfahan University of Technology, Isfahan, Iran

H. Bakhshiansohi^{45,46} , E. Khazaie⁴⁶, M. Zeinali⁴⁷

Institute for Research in Fundamental Sciences (IPM), Tehran, Iran

S. Chenarani⁴⁸, S.M. Etesami , M. Khakzad , M. Mohammadi Najafabadi 

University College Dublin, Dublin, Ireland

M. Grunewald 

INFN Sezione di Bari ^a, Bari, Italy, Università di Bari ^b, Bari, Italy, Politecnico di Bari ^c, Bari, Italy

M. Abbrescia^{a,b} , R. Aly^{a,b,49} , C. Aruta^{a,b}, A. Colaleo^a , D. Creanza^{a,c} , N. De Filippis^{a,c} , M. De Palma^{a,b} , A. Di Florio^{a,b}, A. Di Pilato^{a,b} , W. Elmetenawee^{a,b} , F. Errico^{a,b} , L. Fiore^a , A. Gelmi^{a,b} , G. Iaselli^{a,c} , M. Ince^{a,b} , S. Lezki^{a,b} , G. Maggi^{a,c} , M. Maggi^a , I. Margjeka^{a,b}, V. Mastrapasqua^{a,b} , S. My^{a,b} , S. Nuzzo^{a,b} , A. Pellecchia^{a,b}, A. Pompili^{a,b} , G. Pugliese^{a,c} , D. Ramos^a, A. Ranieri^a , G. Selvaggi^{a,b} , L. Silvestris^a , F.M. Simone^{a,b} , Ü. Sözbilir^a, R. Venditti^a , P. Verwilligen^a 

INFN Sezione di Bologna ^a, Bologna, Italy, Università di Bologna ^b, Bologna, Italy

G. Abbiendi^a , C. Battilana^{a,b} , D. Bonacorsi^{a,b} , L. Borgonovi^a, L. Brigliadori^a, R. Campanini^{a,b} , P. Capiluppi^{a,b} , A. Castro^{a,b} , F.R. Cavallo^a , C. Ciocca^a , M. Cuffiani^{a,b} , G.M. Dallavalle^a , T. Diotalevi^{a,b} , F. Fabbri^a , A. Fanfani^{a,b} , P. Giacomelli^a , L. Giommi^{a,b} , C. Grandi^a , L. Guiducci^{a,b}, S. Lo Meo^{a,50}, L. Lunerti^{a,b}, S. Marcellini^a , G. Masetti^a , F.L. Navarria^{a,b} , A. Perrotta^a , F. Primavera^{a,b} , A.M. Rossi^{a,b} , T. Rovelli^{a,b} , G.P. Siroli^{a,b} 

INFN Sezione di Catania ^a, Catania, Italy, Università di Catania ^b, Catania, Italy

S. Albergo^{a,b,51} , S. Costa^{a,b,51} , A. Di Mattia^a , R. Potenza^{a,b}, A. Tricomi^{a,b,51} , C. Tuve^{a,b} 

INFN Sezione di Firenze ^a, Firenze, Italy, Università di Firenze ^b, Firenze, Italy

G. Barbagli^a , A. Cassese^a , R. Ceccarelli^{a,b}, V. Ciulli^{a,b} , C. Civinini^a , R. D'Alessandro^{a,b} , E. Focardi^{a,b} , G. Latino^{a,b} , P. Lenzi^{a,b} , M. Lizzo^{a,b}, M. Meschini^a , S. Paoletti^a , R. Seidita^{a,b}, G. Sguazzoni^a , L. Viliani^a 

INFN Laboratori Nazionali di Frascati, Frascati, Italy

L. Benussi , S. Bianco , D. Piccolo 

INFN Sezione di Genova ^a, Genova, Italy, Università di Genova ^b, Genova, Italy

M. Bozzo^{a,b} , F. Ferro^a , R. Mulargia^a, E. Robutti^a , S. Tosi^{a,b} 

INFN Sezione di Milano-Bicocca ^a, Milano, Italy, Università di Milano-Bicocca ^b, Milano, Italy

A. Benaglia^a , G. Boldrini , F. Brivio^{a,b}, F. Cetorelli^{a,b}, F. De Guio^{a,b} , M.E. Dinardo^{a,b} , P. Dini^a , S. Gennai^a , A. Ghezzi^{a,b} , P. Govoni^{a,b} , L. Guzzi^{a,b} , M.T. Lucchini^{a,b} , M. Malberti^a, S. Malvezzi^a , A. Massironi^a , D. Menasce^a , L. Moroni^a , M. Paganoni^{a,b} , D. Pedrini^a , B.S. Pinolini, S. Ragazzi^{a,b} , N. Redaelli^a , T. Tabarelli de Fatis^{a,b} , D. Valsecchi^{a,b,22}, D. Zuolo^{a,b} 

INFN Sezione di Napoli ^a, Napoli, Italy, Università di Napoli 'Federico II' ^b, Napoli, Italy, Università della Basilicata ^c, Potenza, Italy, Università G. Marconi ^d, Roma, Italy

S. Buontempo^a , F. Carnevali^{a,b}, N. Cavallo^{a,c} , A. De Iorio^{a,b} , F. Fabozzi^{a,c} , A.O.M. Iorio^{a,b} , L. Lista^{a,b,52} , S. Meola^{a,d,22} , P. Paolucci^{a,22} , B. Rossi^a , C. Sciacca^{a,b} 

INFN Sezione di Padova ^a, Padova, Italy, Università di Padova ^b, Padova, Italy, Università di Trento ^c, Trento, Italy

P. Azzi^a , N. Bacchetta^a , D. Bisello^{a,b} , P. Bortignon^a , A. Bragagnolo^{a,b} , R. Carlin^{a,b} , P. Checchia^a , T. Dorigo^a , U. Dosselli^a , F. Gasparini^{a,b} , U. Gasparini^{a,b} , G. Grossi, L. Layer^{a,53}, E. Lusiani , M. Margoni^{a,b} 

A.T. Meneguzzo^{a,b} , J. Pazzini^{a,b} , P. Ronchese^{a,b} , R. Rossin^{a,b}, F. Simonetto^{a,b} , G. Strong^a , M. Tosi^{a,b} , H. Yarar^{a,b}, M. Zanetti^{a,b} , P. Zotto^{a,b} , A. Zucchetta^{a,b} , G. Zumerle^{a,b}

INFN Sezione di Pavia ^a, Pavia, Italy, Università di Pavia ^b, Pavia, Italy

C. Aimè^{a,b}, A. Braghieri^a , S. Calzaferri^{a,b}, D. Fiorina^{a,b} , P. Montagna^{a,b}, S.P. Ratti^{a,b}, V. Re^a , C. Riccardi^{a,b} , P. Salvini^a , I. Vai^a , P. Vitulo^{a,b} 

INFN Sezione di Perugia ^a, Perugia, Italy, Università di Perugia ^b, Perugia, Italy

P. Asenov^{a,54} , G.M. Bilei^a , D. Ciangottini^{a,b} , L. Fanò^{a,b} , M. Magherini^b, G. Mantovani^{a,b}, V. Mariani^{a,b}, M. Menichelli^a , F. Moscatelli^{a,54} , A. Piccinelli^{a,b} , M. Presilla^{a,b} , A. Rossi^{a,b} , A. Santocchia^{a,b} , D. Spiga^a , T. Tedeschi^{a,b}

INFN Sezione di Pisa ^a, Pisa, Italy, Università di Pisa ^b, Pisa, Italy, Scuola Normale Superiore di Pisa ^c, Pisa, Italy, Università di Siena ^d, Siena, Italy

P. Azzurri^a , G. Bagliesi^a , V. Bertacchi^{a,c} , L. Bianchini^a , T. Boccali^a , E. Bossini^{a,b} , R. Castaldi^a , M.A. Ciocci^{a,b} , V. D'Amante^{a,d} , R. Dell'Orso^a , M.R. Di Domenico^{a,d} , S. Donato^a , A. Giassi^a , F. Ligabue^{a,c} , E. Manca^{a,c} , G. Mandorli^{a,c} , D. Matos Figueiredo, A. Messineo^{a,b} , M. Musich^a, F. Palla^a , S. Parolia^{a,b}, G. Ramirez-Sánchez^{a,c}, A. Rizzi^{a,b} , G. Rolandi^{a,c} , S. Roy Chowdhury^{a,c}, A. Scribano^a, N. Shafiei^{a,b} , P. Spagnolo^a , R. Tenchini^a , G. Tonelli^{a,b} , N. Turini^{a,d} , A. Venturi^a , P.G. Verdini^a

INFN Sezione di Roma ^a, Rome, Italy, Sapienza Università di Roma ^b, Rome, Italy

P. Barria^a , M. Campana^{a,b}, F. Cavallari^a , D. Del Re^{a,b} , E. Di Marco^a , M. Diemoz^a , E. Longo^{a,b} , P. Meridiani^a , G. Organtini^{a,b} , F. Pandolfi^a, R. Paramatti^{a,b} , C. Quaranta^{a,b}, S. Rahatlou^{a,b} , C. Rovelli^a , F. Santanastasio^{a,b} , L. Soffi^a , R. Tramontano^{a,b}

INFN Sezione di Torino ^a, Torino, Italy, Università di Torino ^b, Torino, Italy, Università del Piemonte Orientale ^c, Novara, Italy

N. Amapane^{a,b} , R. Arcidiacono^{a,c} , S. Argiro^{a,b} , M. Arneodo^{a,c} , N. Bartosik^a , R. Bellan^{a,b} , A. Bellora^{a,b} , J. Berenguer Antequera^{a,b} , C. Biino^a , N. Cartiglia^a , M. Costa^{a,b} , R. Covarelli^{a,b} , N. Demaria^a , B. Kiani^{a,b} , F. Legger^a , C. Mariotti^a , S. Maselli^a , E. Migliore^{a,b} , E. Monteil^{a,b} , M. Monteno^a , M.M. Obertino^{a,b} , G. Ortona^a , L. Pacher^{a,b} , N. Pastrone^a , M. Pelliccioni^a , M. Ruspa^{a,c} , K. Shchelina^a , F. Siviero^{a,b} , V. Sola^a , A. Solano^{a,b} , D. Soldi^{a,b} , A. Staiano^a , M. Tornago^{a,b}, D. Trocino^a , A. Vagnerini^{a,b}

INFN Sezione di Trieste ^a, Trieste, Italy, Università di Trieste ^b, Trieste, Italy

S. Belforte^a , V. Cadelise^{a,b} , M. Casarsa^a , F. Cossutti^a , A. Da Rold^{a,b} , G. Della Ricca^{a,b} , G. Sorrentino^{a,b}

Kyungpook National University, Daegu, Korea

S. Dogra , C. Huh , B. Kim, D.H. Kim , G.N. Kim , J. Kim, J. Lee, S.W. Lee , C.S. Moon , Y.D. Oh , S.I. Pak, S. Sekmen , Y.C. Yang

Chonnam National University, Institute for Universe and Elementary Particles, Kwangju, Korea

H. Kim , D.H. Moon 

Hanyang University, Seoul, Korea

B. Francois , T.J. Kim , J. Park 

Korea University, Seoul, Korea

S. Cho, S. Choi , B. Hong , K. Lee, K.S. Lee , J. Lim, J. Park, S.K. Park, J. Yoo

Kyung Hee University, Department of Physics, Seoul, Republic of Korea, Seoul, Korea
J. Goh , A. Gurtu

Sejong University, Seoul, Korea
H.S. Kim , Y. Kim

Seoul National University, Seoul, Korea

J. Almond, J.H. Bhyun, J. Choi, S. Jeon, J. Kim, J.S. Kim, S. Ko, H. Kwon, H. Lee , S. Lee, B.H. Oh, M. Oh , S.B. Oh, H. Seo , U.K. Yang, I. Yoon 

University of Seoul, Seoul, Korea

W. Jang, D.Y. Kang, Y. Kang, S. Kim, B. Ko, J.S.H. Lee , Y. Lee, J.A. Merlin, I.C. Park, Y. Roh, M.S. Ryu, D. Song, I.J. Watson , S. Yang

Yonsei University, Department of Physics, Seoul, Korea

S. Ha, H.D. Yoo

Sungkyunkwan University, Suwon, Korea

M. Choi, H. Lee, Y. Lee, I. Yu 

College of Engineering and Technology, American University of the Middle East (AUM), Egaila, Kuwait, Dasman, Kuwait

T. Beyrouthy, Y. Maghrbi

Riga Technical University, Riga, Latvia

K. Dreimanis , V. Veckalns⁵⁵ 

Vilnius University, Vilnius, Lithuania

M. Ambrozas, A. Carvalho Antunes De Oliveira , A. Juodagalvis , A. Rinkevicius , G. Tamulaitis 

National Centre for Particle Physics, Universiti Malaya, Kuala Lumpur, Malaysia

N. Bin Norjoharuddeen , Z. Zolkapli

Universidad de Sonora (UNISON), Hermosillo, Mexico

J.F. Benitez , A. Castaneda Hernandez , H.A. Encinas Acosta, L.G. Gallegos Maríñez, M. León Coello, J.A. Murillo Quijada , A. Sehrawat, L. Valencia Palomo 

Centro de Investigacion y de Estudios Avanzados del IPN, Mexico City, Mexico

G. Ayala, H. Castilla-Valdez, E. De La Cruz-Burelo , I. Heredia-De La Cruz⁵⁶ , R. Lopez-Fernandez, C.A. Mondragon Herrera, D.A. Perez Navarro, R. Reyes-Almanza , A. Sánchez Hernández 

Universidad Iberoamericana, Mexico City, Mexico

S. Carrillo Moreno, C. Oropeza Barrera , F. Vazquez Valencia

Benemerita Universidad Autonoma de Puebla, Puebla, Mexico

I. Pedraza, H.A. Salazar Ibarguen, C. Uribe Estrada

University of Montenegro, Podgorica, Montenegro

J. Mijuskovic⁵⁷, N. Raicevic

University of Auckland, Auckland, New Zealand

D. Krovcheck 

University of Canterbury, Christchurch, New Zealand

P.H. Butler 

National Centre for Physics, Quaid-I-Azam University, Islamabad, Pakistan

A. Ahmad, M.I. Asghar, A. Awais, M.I.M. Awan, M. Gul , H.R. Hoorani, W.A. Khan, M.A. Shah, M. Shoib , M. Waqas 

AGH University of Science and Technology Faculty of Computer Science, Electronics and Telecommunications, Krakow, Poland

V. Avati, L. Grzanka, M. Malawski

National Centre for Nuclear Research, Swierk, Poland

H. Bialkowska, M. Bluj , B. Boimska , M. Górski, M. Kazana, M. Szleper , P. Zalewski

Institute of Experimental Physics, Faculty of Physics, University of Warsaw, Warsaw, Poland

K. Bunkowski, K. Doroba, A. Kalinowski , M. Konecki , J. Krolikowski 

Laboratório de Instrumentação e Física Experimental de Partículas, Lisboa, Portugal

M. Araujo, P. Bargassa , D. Bastos, A. Boletti , P. Faccioli , M. Gallinaro , J. Hollar , N. Leonardo , T. Niknejad, M. Pisano, J. Seixas , O. Toldaiev , J. Varela 

Joint Institute for Nuclear Research, Dubna, Russia

S. Afanasiev, D. Budkouski, I. Golutvin, I. Gorbunov , V. Karjavine, V. Korenkov , A. Lanev, A. Malakhov, V. Matveev^{58,59}, V. Palichik, V. Perelygin, M. Savina, V. Shalaev, S. Shmatov, S. Shulha, V. Smirnov, O. Teryaev, N. Voytishin, B.S. Yuldashev⁶⁰, A. Zarubin, I. Zhizhin

Petersburg Nuclear Physics Institute, Gatchina (St. Petersburg), Russia

G. Gavrilov , V. Golovtcov, Y. Ivanov, V. Kim⁶¹ , E. Kuznetsova⁶² , V. Murzin, V. Oreshkin, I. Smirnov, D. Sosnov , V. Sulimov, L. Uvarov, S. Volkov, A. Vorobyev

Institute for Nuclear Research, Moscow, Russia

Yu. Andreev , A. Dermenev, S. Gninenko , N. Golubev, A. Karneyeu , D. Kirpichnikov , M. Kirsanov, N. Krasnikov, A. Pashenkov, G. Pivovarov , A. Toropin

Moscow Institute of Physics and Technology, Moscow, Russia

T. Aushev

National Research Center 'Kurchatov Institute', Moscow, Russia

V. Epshteyn, V. Gavrilov, N. Lychkovskaya, A. Nikitenko⁶³, V. Popov, A. Stepenov, M. Toms, E. Vlasov , A. Zhokin

National Research Nuclear University 'Moscow Engineering Physics Institute' (MEPhI), Moscow, Russia

M. Chadeeva⁶⁴ , A. Osokin, P. Parygin, E. Popova, V. Rusinov, D. Selivanova

P.N. Lebedev Physical Institute, Moscow, Russia

V. Andreev, M. Azarkin, I. Dremin , M. Kirakosyan, A. Terkulov

Skobeltsyn Institute of Nuclear Physics, Lomonosov Moscow State University, Moscow, Russia

A. Belyaev, E. Boos , V. Bunichev, M. Dubinin⁶⁵ , L. Dudko , V. Klyukhin , O. Kodolova , I. Lokhtin , O. Lukina, S. Obraztsov, S. Petrushanko, V. Savrin, A. Snigirev 

Novosibirsk State University (NSU), Novosibirsk, Russia

V. Blinov⁶⁶, T. Dimova⁶⁶, L. Kardapoltsev⁶⁶, A. Kozyrev⁶⁶, I. Ovtin⁶⁶, O. Radchenko⁶⁶, Y. Skovpen⁶⁶ 

Institute for High Energy Physics of National Research Centre 'Kurchatov Institute',

Protvino, Russia

I. Azhgirey , I. Bayshev, D. Elumakhov, V. Kachanov, D. Konstantinov , P. Mandrik , V. Petrov, R. Ryutin, S. Slabospitskii , A. Sobol, S. Troshin , N. Tyurin, A. Uzunian, A. Volkov

National Research Tomsk Polytechnic University, Tomsk, Russia

A. Babaev, V. Okhotnikov

Tomsk State University, Tomsk, Russia

V. Borshch, V. Ivanchenko , E. Tcherniaev 

University of Belgrade: Faculty of Physics and VINCA Institute of Nuclear Sciences, Belgrade, Serbia

P. Adzic⁶⁷ , M. Dordevic , P. Milenovic , J. Milosevic 

Centro de Investigaciones Energéticas Medioambientales y Tecnológicas (CIEMAT), Madrid, Spain

M. Aguilar-Benitez, J. Alcaraz Maestre , A. Álvarez Fernández, I. Bachiller, M. Barrio Luna, Cristina F. Bedoya , C.A. Carrillo Montoya , M. Cepeda , M. Cerrada, N. Colino , B. De La Cruz, A. Delgado Peris , J.P. Fernández Ramos , J. Flix , M.C. Fouz , O. Gonzalez Lopez , S. Goy Lopez , J.M. Hernandez , M.I. Josa , J. León Holgado , D. Moran, Á. Navarro Tobar , C. Perez Dengra, A. Pérez-Calero Yzquierdo , J. Puerta Pelayo , I. Redondo , L. Romero, S. Sánchez Navas, L. Urda Gómez , C. Willmott

Universidad Autónoma de Madrid, Madrid, Spain

J.F. de Trocóniz

Universidad de Oviedo, Instituto Universitario de Ciencias y Tecnologías Espaciales de Asturias (ICTEA), Oviedo, Spain

B. Alvarez Gonzalez , J. Cuevas , C. Erice , J. Fernandez Menendez , S. Folgueras , I. Gonzalez Caballero , J.R. González Fernández, E. Palencia Cortezon , C. Ramón Álvarez, V. Rodríguez Bouza , A. Soto Rodríguez, A. Trapote, N. Trevisani , C. Vico Villalba

Instituto de Física de Cantabria (IFCA), CSIC-Universidad de Cantabria, Santander, Spain

J.A. Brochero Cifuentes , I.J. Cabrillo, A. Calderon , J. Duarte Campderros , M. Fernandez , C. Fernandez Madrazo , P.J. Fernández Manteca , A. García Alonso, G. Gomez, C. Martinez Rivero, P. Martinez Ruiz del Arbol , F. Matorras , P. Matorras Cuevas , J. Piedra Gomez , C. Prieels, A. Ruiz-Jimeno , L. Scodellaro , I. Vila, J.M. Vizan Garcia 

University of Colombo, Colombo, Sri Lanka

M.K. Jayananda, B. Kailasapathy⁶⁸, D.U.J. Sonnadara, D.D.C. Wickramarathna

University of Ruhuna, Department of Physics, Matara, Sri Lanka

W.G.D. Dharmaratna , K. Liyanage, N. Perera, N. Wickramage

CERN, European Organization for Nuclear Research, Geneva, Switzerland

T.K. Aarrestad , D. Abbaneo, J. Alimena , E. Auffray, G. Auzinger, J. Baechler, P. Baillon[†], D. Barney , J. Bendavid, M. Bianco , A. Bocci , C. Caillol, T. Camporesi, M. Capeans Garrido , G. Cerminara, N. Chernyavskaya , S.S. Chhibra , S. Choudhury, M. Cipriani , L. Cristella , D. d'Enterria , A. Dabrowski , A. David , A. De Roeck , M.M. Defranchis , M. Deile , M. Dobson, M. Dünser , N. Dupont, A. Elliott-Peisert, F. Fallavollita⁶⁹, A. Florent , L. Forthomme , G. Franzoni , W. Funk, S. Ghosh , S. Giani, D. Gigi, K. Gill, F. Glege, L. Gouskos , E. Govorkova , M. Haranko , J. Hegeman , V. Innocente , T. James, P. Janot , J. Kaspar , J. Kieseler , M. Komm , N. Kratochwil, C. Lange , S. Laurila, P. Lecoq , A. Lintuluoto, K. Long , C. Lourenço , B. Maier,

L. Malgeri [id](#), S. Mallios, M. Mannelli, A.C. Marini [id](#), F. Meijers, S. Mersi [id](#), E. Meschi [id](#), F. Moortgat [id](#), M. Mulders [id](#), S. Orfanelli, L. Orsini, F. Pantaleo [id](#), E. Perez, M. Peruzzi [id](#), A. Petrilli, G. Petrucciani [id](#), A. Pfeiffer [id](#), M. Pierini [id](#), D. Piparo, M. Pitt [id](#), H. Qu [id](#), T. Quast, D. Rabady [id](#), A. Racz, G. Reales Gutiérrez, M. Rovere, H. Sakulin, J. Salfeld-Nebgen [id](#), S. Scarfi, C. Schwick, M. Selvaggi [id](#), A. Sharma, P. Silva [id](#), W. Snoeys [id](#), P. Sphicas⁷⁰ [id](#), S. Summers [id](#), K. Tatar [id](#), V.R. Tavolaro [id](#), D. Treille, P. Tropea, A. Tsirou, J. Wanczyk⁷¹, K.A. Wozniak, W.D. Zeuner

Paul Scherrer Institut, Villigen, Switzerland

L. Caminada⁷² [id](#), A. Ebrahimi [id](#), W. Erdmann, R. Horisberger, Q. Ingram, H.C. Kaestli, D. Kotlinski, U. Langenegger, M. Missiroli⁷² [id](#), L. Noehte⁷², T. Rohe

ETH Zurich - Institute for Particle Physics and Astrophysics (IPA), Zurich, Switzerland

K. Androsov⁷¹ [id](#), M. Backhaus [id](#), P. Berger, A. Calandri [id](#), A. De Cosa, G. Dissertori [id](#), M. Dittmar, M. Donegà, C. Dorfer [id](#), F. Eble, K. Gedia, F. Glessgen, T.A. Gómez Espinosa [id](#), C. Grab [id](#), D. Hits, W. Lustermann, A.-M. Lyon, R.A. Manzoni [id](#), L. Marchese [id](#), C. Martin Perez, M.T. Meinhard, F. Nessi-Tedaldi, J. Niedziela [id](#), F. Pauss, V. Perovic, S. Pigazzini [id](#), M.G. Ratti [id](#), M. Reichmann, C. Reissel, T. Reitenspiess, B. Ristic [id](#), D. Ruini, D.A. Sanz Becerra [id](#), V. Stampf, J. Steggemann⁷¹ [id](#), R. Wallny [id](#)

Universität Zürich, Zurich, Switzerland

C. Amsler⁷³ [id](#), P. Bärtschi, C. Botta [id](#), D. Brzhechko, M.F. Canelli [id](#), K. Cormier, A. De Wit [id](#), R. Del Burgo, J.K. Heikkilä [id](#), M. Huwiler, W. Jin, A. Jofrehei [id](#), B. Kilminster [id](#), S. Leontsinis [id](#), S.P. Liechti, A. Macchiolo [id](#), P. Meiring, V.M. Mikuni [id](#), U. Molinatti, I. Neutelings, A. Reimers, P. Robmann, S. Sanchez Cruz [id](#), K. Schweiger [id](#), M. Senger, Y. Takahashi [id](#)

National Central University, Chung-Li, Taiwan

C. Adloff⁷⁴, C.M. Kuo, W. Lin, A. Roy [id](#), T. Sarkar⁴² [id](#), S.S. Yu

National Taiwan University (NTU), Taipei, Taiwan

L. Ceard, Y. Chao, K.F. Chen [id](#), P.H. Chen [id](#), P.s. Chen, H. Cheng [id](#), W.-S. Hou [id](#), Y.y. Li, R.-S. Lu, E. Paganis [id](#), A. Psallidas, A. Steen, H.y. Wu, E. Yazgan [id](#), P.r. Yu

Chulalongkorn University, Faculty of Science, Department of Physics, Bangkok, Thailand

B. Asavapibhop [id](#), C. Asawatangtrakuldee [id](#), N. Srimanobhas [id](#)

Çukurova University, Physics Department, Science and Art Faculty, Adana, Turkey

F. Boran [id](#), S. Damarseckin⁷⁵, Z.S. Demiroglu [id](#), F. Dolek [id](#), I. Dumanoglu⁷⁶ [id](#), E. Eskut, Y. Guler⁷⁷ [id](#), E. Gurpinar Guler⁷⁷ [id](#), C. Isik, O. Kara, A. Kayis Topaksu, U. Kiminsu [id](#), G. Onengut, K. Ozdemir⁷⁸, A. Polatoz, A.E. Simsek [id](#), B. Tali⁷⁹, U.G. Tok [id](#), S. Turkcapar, I.S. Zorbakir [id](#)

Middle East Technical University, Physics Department, Ankara, Turkey

G. Karapinar, K. Ocalan⁸⁰ [id](#), M. Yalvac⁸¹ [id](#)

Bogazici University, Istanbul, Turkey

B. Akgun, I.O. Atakisi [id](#), E. Gulmez [id](#), M. Kaya⁸² [id](#), O. Kaya⁸³, Ö. Özçelik, S. Tekten⁸⁴, E.A. Yetkin⁸⁵ [id](#)

Istanbul Technical University, Istanbul, Turkey

A. Cakir [id](#), K. Cankocak⁷⁶ [id](#), Y. Komurcu, S. Sen⁸⁶ [id](#)

Istanbul University, Istanbul, Turkey

S. Cerci⁷⁹, I. Hos⁸⁷, B. Isildak⁸⁸, B. Kaynak, S. Ozkorucuklu, H. Sert [id](#), C. Simsek,

D. Sunar Cerci⁷⁹ , C. Zorbilmez

Institute for Scintillation Materials of National Academy of Science of Ukraine, Kharkov, Ukraine

B. Grynyov

National Scientific Center, Kharkov Institute of Physics and Technology, Kharkov, Ukraine
L. Levchuk 

University of Bristol, Bristol, United Kingdom

D. Anthony, E. Bhal , S. Bologna, J.J. Brooke , A. Bundock , E. Clement , D. Cussans , H. Flacher , J. Goldstein , G.P. Heath, H.F. Heath , L. Kreczko , B. Krikler , S. Paramesvaran, S. Seif El Nasr-Storey, V.J. Smith, N. Stylianou⁸⁹ , K. Walkingshaw Pass, R. White

Rutherford Appleton Laboratory, Didcot, United Kingdom

K.W. Bell, A. Belyaev⁹⁰ , C. Brew , R.M. Brown, D.J.A. Cockerill, C. Cooke, K.V. Ellis, K. Harder, S. Harper, M.-L. Holmberg⁹¹, J. Linacre , K. Manolopoulos, D.M. Newbold , E. Olaiya, D. Petyt, T. Reis , T. Schuh, C.H. Shepherd-Themistocleous, I.R. Tomalin, T. Williams 

Imperial College, London, United Kingdom

R. Bainbridge , P. Bloch , S. Bonomally, J. Borg , S. Breeze, O. Buchmuller, V. Cepaitis , G.S. Chahal⁹² , D. Colling, P. Dauncey , G. Davies , M. Della Negra , S. Fayer, G. Fedi , G. Hall , M.H. Hassanshahi, G. Iles, J. Langford, L. Lyons, A.-M. Magnan, S. Malik, A. Martelli , D.G. Monk, J. Nash⁹³ , M. Pesaresi, B.C. Radburn-Smith, D.M. Raymond, A. Richards, A. Rose, E. Scott , C. Seez, A. Shtipliyski, A. Tapper , K. Uchida, T. Virdee²² , M. Vojinovic , N. Wardle , S.N. Webb , D. Winterbottom

Brunel University, Uxbridge, United Kingdom

K. Coldham, J.E. Cole , A. Khan, P. Kyberd , I.D. Reid , L. Teodorescu, S. Zahid 

Baylor University, Waco, Texas, USA

S. Abdullin , A. Brinkerhoff , B. Caraway , J. Dittmann , K. Hatakeyama , A.R. Kanuganti, B. McMaster , M. Saunders , S. Sawant, C. Sutantawibul, J. Wilson 

Catholic University of America, Washington, DC, USA

R. Bartek , A. Dominguez , R. Uniyal , A.M. Vargas Hernandez

The University of Alabama, Tuscaloosa, Alabama, USA

A. Buccilli , S.I. Cooper , D. Di Croce , S.V. Gleyzer , C. Henderson , C.U. Perez , P. Rumerio⁹⁴ , C. West 

Boston University, Boston, Massachusetts, USA

A. Akpinar , A. Albert , D. Arcaro , C. Cosby , Z. Demiragli , E. Fontanesi, D. Gastler, S. May , J. Rohlf , K. Salyer , D. Sperka, D. Spitzbart , I. Suarez , A. Tsatsos, S. Yuan, D. Zou

Brown University, Providence, Rhode Island, USA

G. Benelli , B. Burkle , X. Coubez²³, D. Cutts , M. Hadley , U. Heintz , J.M. Hogan⁹⁵ , T. Kwon, G. Landsberg , K.T. Lau , D. Li, M. Lukasik, J. Luo , M. Narain, N. Pervan, S. Sagir⁹⁶ , F. Simpson, E. Usai , W.Y. Wong, X. Yan , D. Yu , W. Zhang

University of California, Davis, Davis, California, USA

J. Bonilla , C. Brainerd , R. Breedon, M. Calderon De La Barca Sanchez, M. Chertok 

J. Conway , P.T. Cox, R. Erbacher, G. Haza, F. Jensen , O. Kukral, R. Lander, M. Mulhearn , D. Pellett, B. Regnery , D. Taylor , Y. Yao , F. Zhang

University of California, Los Angeles, California, USA

M. Bachtis , R. Cousins , A. Datta , D. Hamilton, J. Hauser , M. Ignatenko, M.A. Iqbal, T. Lam, W.A. Nash, S. Regnard , D. Saltzberg , B. Stone, V. Valuev

University of California, Riverside, Riverside, California, USA

Y. Chen, R. Clare , J.W. Gary , M. Gordon, G. Hanson , G. Karapostoli , O.R. Long , N. Manganelli, W. Si , S. Wimpenny, Y. Zhang

University of California, San Diego, La Jolla, California, USA

J.G. Branson, P. Chang , S. Cittolin, S. Cooperstein , N. Deelen , D. Diaz , J. Duarte , R. Gerosa , L. Giannini , J. Guiang, R. Kansal , V. Krutelyov , R. Lee, J. Letts , M. Masciovecchio , F. Mokhtar, M. Pieri , B.V. Sathia Narayanan , V. Sharma , M. Tadel, F. Würthwein , Y. Xiang , A. Yagil

University of California, Santa Barbara - Department of Physics, Santa Barbara, California, USA

N. Amin, C. Campagnari , M. Citron , G. Collura , A. Dorsett, V. Dutta , J. Incandela , M. Kilpatrick , J. Kim , B. Marsh, H. Mei, M. Oshiro, M. Quinnan , J. Richman, U. Sarica , F. Setti, J. Sheplock, P. Siddireddy, D. Stuart, S. Wang

California Institute of Technology, Pasadena, California, USA

A. Bornheim , O. Cerri, I. Dutta , J.M. Lawhorn , N. Lu , J. Mao, H.B. Newman , T.Q. Nguyen , M. Spiropulu , J.R. Vlimant , C. Wang , S. Xie , Z. Zhang , R.Y. Zhu

Carnegie Mellon University, Pittsburgh, Pennsylvania, USA

J. Alison , S. An , M.B. Andrews, P. Bryant , T. Ferguson , A. Harilal, C. Liu, T. Mudholkar , M. Paulini , A. Sanchez, W. Terrill

University of Colorado Boulder, Boulder, Colorado, USA

J.P. Cumalat , W.T. Ford , A. Hassani, G. Karathanasis, E. MacDonald, R. Patel, A. Perloff , C. Savard, N. Schonbeck, K. Stenson , K.A. Ulmer , S.R. Wagner , N. Zipper

Cornell University, Ithaca, New York, USA

J. Alexander , S. Bright-Thonney , X. Chen , Y. Cheng , D.J. Cranshaw , S. Hogan, J. Monroy , J.R. Patterson , D. Quach , J. Reichert , M. Reid , A. Ryd, W. Sun , J. Thom , P. Wittich , R. Zou

Fermi National Accelerator Laboratory, Batavia, Illinois, USA

M. Albrow , M. Alyari , G. Apollinari, A. Apresyan , A. Apyan , L.A.T. Bauerdtick , D. Berry , J. Berryhill , P.C. Bhat, K. Burkett , J.N. Butler, A. Canepa, G.B. Cerati , H.W.K. Cheung , F. Chlebana, K.F. Di Petrillo , J. Dickinson , V.D. Elvira , Y. Feng, J. Freeman, Z. Gecse, L. Gray, D. Green, S. Grünendahl , O. Gutsche , R.M. Harris , R. Heller, T.C. Herwig , J. Hirschauer , B. Jayatilaka , S. Jindariani, M. Johnson, U. Joshi, T. Klijnsma , B. Klma , K.H.M. Kwok, S. Lammel , D. Lincoln , R. Lipton, T. Liu, C. Madrid, K. Maeshima, C. Mantilla , D. Mason, P. McBride , P. Merkel, S. Mrenna , S. Nahn , J. Ngadiuba , V. Papadimitriou, N. Pastika, K. Pedro , C. Pena⁶⁵ , F. Ravera , A. Reinsvold Hall⁹⁷ , L. Ristori , E. Sexton-Kennedy , N. Smith , A. Soha , L. Spiegel, S. Stoynev , J. Strait , L. Taylor , S. Tkaczyk, N.V. Tran , L. Uplegger , E.W. Vaandering , H.A. Weber

University of Florida, Gainesville, Florida, USA

P. Avery, D. Bourilkov , L. Cadamuro , V. Cherepanov, R.D. Field, D. Guerrero, M. Kim, E. Koenig, J. Konigsberg , A. Korytov, K.H. Lo, K. Matchev , N. Menendez , G. Mitselmakher , A. Muthirakalayil Madhu, N. Rawal, D. Rosenzweig, S. Rosenzweig, K. Shi , J. Wang , Z. Wu , E. Yigitbasi , X. Zuo

Florida State University, Tallahassee, Florida, USA

T. Adams , A. Askew , R. Habibullah , V. Hagopian, K.F. Johnson, R. Khurana, T. Kolberg , G. Martinez, H. Prosper , C. Schiber, O. Viazlo , R. Yohay , J. Zhang

Florida Institute of Technology, Melbourne, Florida, USA

M.M. Baarmann , S. Butalla, T. Elkafrawy⁹⁸ , M. Hohlmann , R. Kumar Verma , D. Noonan , M. Rahmani, F. Yumiceva 

University of Illinois at Chicago (UIC), Chicago, Illinois, USA

M.R. Adams, H. Becerril Gonzalez , R. Cavanaugh , S. Dittmer, O. Evdokimov , C.E. Gerber , D.J. Hofman , A.H. Merrit, C. Mills , G. Oh , T. Roy, S. Rudrabhatla, M.B. Tonjes , N. Varelas , J. Viinikainen , X. Wang, Z. Ye

The University of Iowa, Iowa City, Iowa, USA

M. Alhusseini , K. Dilsiz⁹⁹ , L. Emediato, R.P. Gandrajula , O.K. Köseyan , J.-P. Merlo, A. Mestvirishvili¹⁰⁰, J. Nachtman, H. Ogul¹⁰¹ , Y. Onel , A. Penzo, C. Snyder, E. Tiras¹⁰² 

Johns Hopkins University, Baltimore, Maryland, USA

O. Amram , B. Blumenfeld , L. Corcodilos , J. Davis, A.V. Gritsan , S. Kyriacou, P. Maksimovic , J. Roskes , M. Swartz, T.Á. Vámi 

The University of Kansas, Lawrence, Kansas, USA

A. Abreu, J. Anguiano, C. Baldenegro Barrera , P. Baringer , A. Bean , Z. Flowers, T. Isidori, S. Khalil , J. King, G. Krintiras , A. Kropivnitskaya , M. Lazarovits, C. Le Mahieu, C. Lindsey, J. Marquez, N. Minafra , M. Murray , M. Nickel, C. Rogan , C. Royon, R. Salvatico , S. Sanders, E. Schmitz, C. Smith , Q. Wang , Z. Warner, J. Williams , G. Wilson

Kansas State University, Manhattan, Kansas, USA

S. Duric, A. Ivanov , K. Kaadze , D. Kim, Y. Maravin , T. Mitchell, A. Modak, K. Nam

Lawrence Livermore National Laboratory, Livermore, California, USA

F. Rebassoo, D. Wright

University of Maryland, College Park, Maryland, USA

E. Adams, A. Baden, O. Baron, A. Belloni , S.C. Eno , N.J. Hadley , S. Jabeen , R.G. Kellogg, T. Koeth, Y. Lai, S. Lascio, A.C. Mignerey, S. Nabili, C. Palmer , M. Seidel , A. Skuja , L. Wang, K. Wong 

Massachusetts Institute of Technology, Cambridge, Massachusetts, USA

D. Abercrombie, G. Andreassi, R. Bi, W. Busza , I.A. Cali, Y. Chen , M. D'Alfonso , J. Eysermans, C. Freer , G. Gomez Ceballos, M. Goncharov, P. Harris, M. Hu, M. Klute , D. Kovalskyi , J. Krupa, Y.-J. Lee , C. Mironov , C. Paus , D. Rankin , C. Roland , G. Roland, Z. Shi , G.S.F. Stephans , J. Wang, Z. Wang , B. Wyslouch

University of Minnesota, Minneapolis, Minnesota, USA

R.M. Chatterjee, A. Evans , J. Hiltbrand, Sh. Jain , B.M. Joshi , M. Krohn, Y. Kubota, J. Mans , M. Revering, R. Rusack , R. Saradhy, N. Schroeder , N. Strobbe , M.A. Wadud

University of Nebraska-Lincoln, Lincoln, Nebraska, USA

K. Bloom [ID](#), M. Bryson, S. Chauhan [ID](#), D.R. Claes, C. Fangmeier, L. Finco [ID](#), F. Golf [ID](#), C. Joo, I. Kravchenko [ID](#), I. Reed, J.E. Siado, G.R. Snow[†], W. Tabb, A. Wightman, F. Yan, A.G. Zecchinelli

State University of New York at Buffalo, Buffalo, New York, USA

G. Agarwal [ID](#), H. Bandyopadhyay [ID](#), L. Hay [ID](#), I. Iashvili [ID](#), A. Kharchilava, C. McLean [ID](#), D. Nguyen, J. Pekkanen [ID](#), S. Rappoccio [ID](#), A. Williams [ID](#)

Northeastern University, Boston, Massachusetts, USA

G. Alverson [ID](#), E. Barberis, Y. Haddad [ID](#), Y. Han, A. Hortiangtham, A. Krishna, J. Li [ID](#), J. Lidrych [ID](#), G. Madigan, B. Marzocchi [ID](#), D.M. Morse [ID](#), V. Nguyen, T. Orimoto [ID](#), A. Parker, L. Skinnari [ID](#), A. Tishelman-Charny, T. Wamorkar, B. Wang [ID](#), A. Wisecarver, D. Wood [ID](#)

Northwestern University, Evanston, Illinois, USA

S. Bhattacharya [ID](#), J. Bueghly, Z. Chen [ID](#), A. Gilbert [ID](#), T. Gunter [ID](#), K.A. Hahn, Y. Liu, N. Odell, M.H. Schmitt [ID](#), M. Velasco

University of Notre Dame, Notre Dame, Indiana, USA

R. Band [ID](#), R. Bucci, M. Cremonesi, A. Das [ID](#), N. Dev [ID](#), R. Goldouzian [ID](#), M. Hildreth, K. Hurtado Anampa [ID](#), C. Jessop [ID](#), K. Lannon [ID](#), J. Lawrence, N. Loukas [ID](#), D. Lutton, J. Mariano, N. Marinelli, I. Mcalister, T. McCauley [ID](#), C. Mcgrady, K. Mohrman, C. Moore, Y. Musienko⁵⁸, R. Ruchti, A. Townsend, M. Wayne, M. Zarucki [ID](#), L. Zygalas

The Ohio State University, Columbus, Ohio, USA

B. Bylsma, L.S. Durkin [ID](#), B. Francis [ID](#), C. Hill [ID](#), M. Nunez Ornelas [ID](#), K. Wei, B.L. Winer, B.R. Yates [ID](#)

Princeton University, Princeton, New Jersey, USA

F.M. Addesa [ID](#), B. Bonham [ID](#), P. Das [ID](#), G. Dezoort, P. Elmer [ID](#), A. Frankenthal [ID](#), B. Greenberg [ID](#), N. Haubrich, S. Higginbotham, A. Kalogeropoulos [ID](#), G. Kopp, S. Kwan [ID](#), D. Lange, D. Marlow [ID](#), K. Mei [ID](#), I. Ojalvo, J. Olsen [ID](#), D. Stickland [ID](#), C. Tully [ID](#)

University of Puerto Rico, Mayaguez, Puerto Rico, USA

S. Malik [ID](#), S. Norberg

Purdue University, West Lafayette, Indiana, USA

A.S. Bakshi, V.E. Barnes [ID](#), R. Chawla [ID](#), S. Das [ID](#), L. Gutay, M. Jones [ID](#), A.W. Jung [ID](#), D. Kondratyev [ID](#), A.M. Koshy, M. Liu, G. Negro, N. Neumeister [ID](#), G. Paspalaki, S. Piperov [ID](#), A. Purohit, J.F. Schulte [ID](#), M. Stojanovic¹⁸, J. Thieman [ID](#), F. Wang [ID](#), R. Xiao [ID](#), W. Xie [ID](#)

Purdue University Northwest, Hammond, Indiana, USA

J. Dolen [ID](#), N. Parashar

Rice University, Houston, Texas, USA

D. Acosta [ID](#), A. Baty [ID](#), T. Carnahan, M. Decaro, S. Dildick [ID](#), K.M. Ecklund [ID](#), S. Freed, P. Gardner, F.J.M. Geurts [ID](#), A. Kumar [ID](#), W. Li, B.P. Padley [ID](#), R. Redjimi, J. Rotter, W. Shi [ID](#), A.G. Stahl Leiton [ID](#), S. Yang [ID](#), L. Zhang¹⁰³, Y. Zhang [ID](#)

University of Rochester, Rochester, New York, USA

A. Bodek [ID](#), P. de Barbaro, R. Demina [ID](#), J.L. Dulemba [ID](#), C. Fallon, T. Ferbel [ID](#), M. Galanti, A. Garcia-Bellido [ID](#), O. Hindrichs [ID](#), A. Khukhunaishvili, E. Ranken, R. Taus, G.P. Van Onsem [ID](#)

Rutgers, The State University of New Jersey, Piscataway, New Jersey, USA

B. Chiarito, J.P. Chou [ID](#), A. Gandrakota [ID](#), Y. Gershtein [ID](#), E. Halkiadakis [ID](#), A. Hart, M. Heindl [ID](#), O. Karacheban²⁶ [ID](#), I. Laflotte, A. Lath [ID](#), R. Montalvo, K. Nash, M. Osherson,

S. Salur , S. Schnetzer, S. Somalwar , R. Stone, S.A. Thayil , S. Thomas, H. Wang 

University of Tennessee, Knoxville, Tennessee, USA

H. Acharya, A.G. Delannoy , S. Fiorendi , S. Spanier 

Texas A&M University, College Station, Texas, USA

O. Bouhali¹⁰⁴ , M. Dalchenko , A. Delgado , R. Eusebi, J. Gilmore, T. Huang, T. Kamon¹⁰⁵, H. Kim , S. Luo , S. Malhotra, R. Mueller, D. Overton, D. Rathjens , A. Safonov 

Texas Tech University, Lubbock, Texas, USA

N. Akchurin, J. Damgov, V. Hegde, S. Kunori, K. Lamichhane, S.W. Lee , T. Mengke, S. Muthumuni , T. Peltola , I. Volobouev, Z. Wang, A. Whitbeck

Vanderbilt University, Nashville, Tennessee, USA

E. Appelt , S. Greene, A. Gurrola , W. Johns, A. Melo, K. Padeken , F. Romeo , P. Sheldon , S. Tuo, J. Velkovska 

University of Virginia, Charlottesville, Virginia, USA

M.W. Arenton , B. Cardwell, B. Cox , G. Cummings , J. Hakala , R. Hirosky , M. Joyce , A. Ledovskoy , A. Li, C. Neu , C.E. Perez Lara , B. Tannenwald , S. White 

Wayne State University, Detroit, Michigan, USA

N. Poudyal 

University of Wisconsin - Madison, Madison, WI, Wisconsin, USA

S. Banerjee, K. Black , T. Bose , S. Dasu , I. De Bruyn , P. Everaerts , C. Galloni, H. He, M. Herndon , A. Herve, U. Hussain, A. Lanaro, A. Loeliger, R. Loveless, J. Madhusudanan Sreekala , A. Mallampalli, A. Mohammadi, D. Pinna, A. Savin, V. Shang, V. Sharma , W.H. Smith , D. Teague, S. Trembath-Reichert, W. Vetens 

†: Deceased

- 1: Also at TU Wien, Wien, Austria
- 2: Also at Institute of Basic and Applied Sciences, Faculty of Engineering, Arab Academy for Science, Technology and Maritime Transport, Alexandria, Egypt
- 3: Also at Université Libre de Bruxelles, Bruxelles, Belgium
- 4: Also at Universidade Estadual de Campinas, Campinas, Brazil
- 5: Also at Federal University of Rio Grande do Sul, Porto Alegre, Brazil
- 6: Also at The University of the State of Amazonas, Manaus, Brazil
- 7: Also at University of Chinese Academy of Sciences, Beijing, China
- 8: Also at Department of Physics, Tsinghua University, Beijing, China
- 9: Also at UFMS, Nova Andradina, Brazil
- 10: Also at Nanjing Normal University Department of Physics, Nanjing, China
- 11: Now at The University of Iowa, Iowa City, Iowa, USA
- 12: Also at National Research Center 'Kurchatov Institute', Moscow, Russia
- 13: Also at Joint Institute for Nuclear Research, Dubna, Russia
- 14: Also at Helwan University, Cairo, Egypt
- 15: Now at Zewail City of Science and Technology, Zewail, Egypt
- 16: Also at Suez University, Suez, Egypt
- 17: Now at British University in Egypt, Cairo, Egypt
- 18: Also at Purdue University, West Lafayette, Indiana, USA
- 19: Also at Université de Haute Alsace, Mulhouse, France
- 20: Also at Tbilisi State University, Tbilisi, Georgia
- 21: Also at Erzincan Binali Yildirim University, Erzincan, Turkey

- 22: Also at CERN, European Organization for Nuclear Research, Geneva, Switzerland
23: Also at RWTH Aachen University, III. Physikalisches Institut A, Aachen, Germany
24: Also at University of Hamburg, Hamburg, Germany
25: Also at Isfahan University of Technology, Isfahan, Iran
26: Also at Brandenburg University of Technology, Cottbus, Germany
27: Also at Forschungszentrum Jülich, Juelich, Germany
28: Also at Physics Department, Faculty of Science, Assiut University, Assiut, Egypt
29: Also at Karoly Robert Campus, MATE Institute of Technology, Gyongyos, Hungary
30: Also at Institute of Physics, University of Debrecen, Debrecen, Hungary
31: Also at Institute of Nuclear Research ATOMKI, Debrecen, Hungary
32: Now at Universitatea Babes-Bolyai - Facultatea de Fizica, Cluj-Napoca, Romania
33: Also at MTA-ELTE Lendület CMS Particle and Nuclear Physics Group, Eötvös Loránd University, Budapest, Hungary
34: Also at Faculty of Informatics, University of Debrecen, Debrecen, Hungary
35: Also at Wigner Research Centre for Physics, Budapest, Hungary
36: Also at IIT Bhubaneswar, Bhubaneswar, India
37: Also at Institute of Physics, Bhubaneswar, India
38: Also at Punjab Agricultural University, Ludhiana, India
39: Also at UPES - University of Petroleum and Energy Studies, Dehradun, India
40: Also at Shoolini University, Solan, India
41: Also at University of Hyderabad, Hyderabad, India
42: Also at University of Visva-Bharati, Santiniketan, India
43: Also at Indian Institute of Science (IISc), Bangalore, India
44: Also at Indian Institute of Technology (IIT), Mumbai, India
45: Also at Deutsches Elektronen-Synchrotron, Hamburg, Germany
46: Now at Department of Physics, Isfahan University of Technology, Isfahan, Iran
47: Also at Sharif University of Technology, Tehran, Iran
48: Also at Department of Physics, University of Science and Technology of Mazandaran, Behshahr, Iran
49: Now at INFN Sezione di Bari, Università di Bari, Politecnico di Bari, Bari, Italy
50: Also at Italian National Agency for New Technologies, Energy and Sustainable Economic Development, Bologna, Italy
51: Also at Centro Siciliano di Fisica Nucleare e di Struttura Della Materia, Catania, Italy
52: Also at Scuola Superiore Meridionale, Università di Napoli Federico II, Napoli, Italy
53: Also at Università di Napoli 'Federico II', Napoli, Italy
54: Also at Consiglio Nazionale delle Ricerche - Istituto Officina dei Materiali, Perugia, Italy
55: Also at Riga Technical University, Riga, Latvia
56: Also at Consejo Nacional de Ciencia y Tecnología, Mexico City, Mexico
57: Also at IRFU, CEA, Université Paris-Saclay, Gif-sur-Yvette, France
58: Also at Institute for Nuclear Research, Moscow, Russia
59: Now at National Research Nuclear University 'Moscow Engineering Physics Institute' (MEPhI), Moscow, Russia
60: Also at Institute of Nuclear Physics of the Uzbekistan Academy of Sciences, Tashkent, Uzbekistan
61: Also at St. Petersburg Polytechnic University, St. Petersburg, Russia
62: Also at University of Florida, Gainesville, Florida, USA
63: Also at Imperial College, London, United Kingdom
64: Also at P.N. Lebedev Physical Institute, Moscow, Russia
65: Also at California Institute of Technology, Pasadena, California, USA

- 66: Also at Budker Institute of Nuclear Physics, Novosibirsk, Russia
67: Also at Faculty of Physics, University of Belgrade, Belgrade, Serbia
68: Also at Trincomalee Campus, Eastern University, Sri Lanka, Nilaveli, Sri Lanka
69: Also at INFN Sezione di Pavia, Università di Pavia, Pavia, Italy
70: Also at National and Kapodistrian University of Athens, Athens, Greece
71: Also at Ecole Polytechnique Fédérale Lausanne, Lausanne, Switzerland
72: Also at Universität Zürich, Zurich, Switzerland
73: Also at Stefan Meyer Institute for Subatomic Physics, Vienna, Austria
74: Also at Laboratoire d'Annecy-le-Vieux de Physique des Particules, IN2P3-CNRS, Annecy-le-Vieux, France
75: Also at Şırnak University, Sirnak, Turkey
76: Also at Near East University, Research Center of Experimental Health Science, Nicosia, Turkey
77: Also at Konya Technical University, Konya, Turkey
78: Also at Piri Reis University, Istanbul, Turkey
79: Also at Adiyaman University, Adiyaman, Turkey
80: Also at Necmettin Erbakan University, Konya, Turkey
81: Also at Bozok Universitetesi Rektörlüğü, Yozgat, Turkey
82: Also at Marmara University, Istanbul, Turkey
83: Also at Milli Savunma University, Istanbul, Turkey
84: Also at Kafkas University, Kars, Turkey
85: Also at İstanbul Bilgi University, İstanbul, Turkey
86: Also at Hacettepe University, Ankara, Turkey
87: Also at İstanbul University - Cerrahpasa, Faculty of Engineering, İstanbul, Turkey
88: Also at Ozyegin University, İstanbul, Turkey
89: Also at Vrije Universiteit Brussel, Brussel, Belgium
90: Also at School of Physics and Astronomy, University of Southampton, Southampton, United Kingdom
91: Also at Rutherford Appleton Laboratory, Didcot, United Kingdom
92: Also at IPPP Durham University, Durham, United Kingdom
93: Also at Monash University, Faculty of Science, Clayton, Australia
94: Also at Università di Torino, Torino, Italy
95: Also at Bethel University, St. Paul, Minneapolis, USA
96: Also at Karamanoğlu Mehmetbey University, Karaman, Turkey
97: Also at United States Naval Academy, Annapolis, N/A, USA
98: Also at Ain Shams University, Cairo, Egypt
99: Also at Bingol University, Bingol, Turkey
100: Also at Georgian Technical University, Tbilisi, Georgia
101: Also at Sinop University, Sinop, Turkey
102: Also at Erciyes University, Kayseri, Turkey
103: Also at Institute of Modern Physics and Key Laboratory of Nuclear Physics and Ion-beam Application (MOE) - Fudan University, Shanghai, China
104: Also at Texas A&M University at Qatar, Doha, Qatar
105: Also at Kyungpook National University, Daegu, Korea